

1 **Mapping Global Non-Floodplain Wetlands**

2

3 Charles R. Lane¹, Ellen D’Amico², Jay R. Christensen^{3,*}, Heather E. Golden^{3,*}, Qiusheng Wu⁴, and
4 Adnan Rajib⁵

5

6 ¹ U.S. Environmental Protection Agency, Office of Research and Development, Center for Environmental
7 Measurement and Modeling, Athens, Georgia, United States of America

8 ² Pegasus Corporation c/o U.S. Environmental Protection Agency, Office of Research and Development,
9 Cincinnati, Ohio, United States of America

10 ³ U.S. Environmental Protection Agency, Office of Research and Development, Center for Environmental
11 Measurement and Modeling, Cincinnati, Ohio, United States of America

12 ⁴ Department of Geography & Sustainability, University of Tennessee, Knoxville, Tennessee, United
13 States of America

14 ⁵ Hydrology and Hydroinformatics Innovation Lab, Department of Civil Engineering, University of Texas
15 at Arlington, Arlington, Texas, United States of America

16

17 * These authors contributed equally to this work

18

19 **Correspondence:** Charles Lane (lane.charles@epa.gov) and Ellen D’Amico (damico.ellen@epa.gov)

20

21 **Abstract.** Non-floodplain wetlands – those located outside the floodplains – have emerged as integral
22 components to watershed resilience, contributing hydrologic and biogeochemical functions affecting
23 watershed-scale flooding extent, drought magnitude, and water-quality maintenance. However, the
24 absence of a global dataset of non-floodplain wetlands limits their necessary incorporation into water
25 quality and quantity management decisions and affects wetland-focused wildlife habitat conservation

26 outcomes. We addressed this critical need by developing a publicly available Global NFW (non-
27 floodplain wetland) dataset, comprised of a global river-floodplain map at 90 m resolution coupled with a
28 global ensemble wetland map incorporating multiple wetland-focused data layers. The floodplain,
29 wetland, and non-floodplain wetland spatial data developed here were successfully validated within 21
30 large and heterogenous basins across the conterminous United States. We identified nearly 33 million
31 potential non-floodplain wetlands with an estimated global extent of over 16 million km². Non-floodplain
32 wetland pixels comprised 53% of globally identified wetland pixels, meaning the majority of the globe's
33 wetlands likely occur external to river floodplains and coastal habitats. The identified Global NFWs were
34 typically small (median 0.039 km²), with a global median size ranging from 0.018-0.138 km². This novel
35 geospatial Global NFW static dataset advances wetland conservation and resource-management goals
36 while providing a foundation for global non-floodplain wetland functional assessments, facilitating non-
37 floodplain wetland inclusion in hydrological, biogeochemical, and biological model development. The
38 data are freely available through the United States Environmental Protection Agency's Environmental
39 Dataset Gateway (https://gaftp.epa.gov/EPADDataCommons/ORD/Global_NonFloodplain_Wetlands/) and
40 through <https://doi.org/10.23719/1528331> (Lane et al., 2023).

41

42 **1 Introduction**

43

44 Wetlands are recognized as globally important ecosystems providing functions leading to critical
45 provisioning (e.g., food, fresh water for domestic, agricultural, and industrial use) and regulating services
46 (e.g., flood and drought mitigation, water purification and waste treatment, and habitat; Millennium
47 Ecosystem Assessment, 2005). Despite their functional importance, wetlands are threatened worldwide by
48 myriad anthropogenic disturbances, including sea-level rise (IPCC, 2014), drainage and filling (Davidson
49 et al., 2014), water abstraction (Liu et al., 2017), consolidation (McCauley et al., 2015), invasive species
50 (Zedler and Kercher, 2004), and changing precipitation and temperature patterns (Winter, 2000). These
51 widespread and globally prevalent alterations to wetlands affect their functioning, resulting in increased

52 downgradient flooding (Golden et al., 2021), modified stream baseflows (Buttle, 2018), reduced pollution
53 mitigation (Evenson et al., 2018a), and habitat loss (Uden et al., 2015).

54
55 Watershed-scale wetland management is currently hampered by the paucity of accurate and fine-grained
56 maps of wetland location (Creed et al., 2017; Christensen et al., 2022). However, methods to identify
57 existing aquatic systems, including wetlands, that provide functions at global scales have recently
58 emerged, such as the Landsat-based 30 m global surface-water inundation data (Pekel et al., 2016), finer-
59 resolution satellite-based landcover maps (e.g., Zanaga et al., 2021), and groundwater-driven aquatic
60 system characterizations (Fan et al., 2013). In addition, methods utilizing digital elevation models to
61 identify topographic depressions likely to support aquatic systems with characteristic wetland features,
62 such as saturated soils and/or ponded waters, have also regionally proliferated (Wu et al., 2019a; Wu et
63 al., 2019b; Christensen et al., 2022).

64
65 These advancements in mapping wetland location, such as those located within the river floodplain or
66 geographically distal from floodplains, allow resource managers to better incorporate wetland
67 biogeochemical, hydrological, and biological functions and concomitantly ecosystem services into their
68 decision-making efforts. For instance, incorporating *floodplain* wetlands into decision-making advances
69 the wise management and conservation of mapped riparian ecosystems (Tullos, 2018; Kundzewicz et al.,
70 2018). Thus, recognizing the importance of wetlands located within active river floodplains, land-
71 management decisions are being made to quantify the functions and ecosystem services of these wetlands
72 and incorporate them into watershed-scale hydro-ecological decisions (e.g., Makungu and Hughes, 2021;
73 Rajib et al., 2021).

74
75 However, *non-floodplain wetlands* are typically not incorporated into watershed-scale conservation and
76 management planning (e.g., Sullivan et al., 2019), thereby ignoring their contributions to watershed-scale
77 resilience in response to biogeochemical and hydrological disturbances (Rains et al., 2016; Golden et al.,

78 2021; Lane et al., 2022). Non-floodplain wetlands are abundant inland freshwater wetlands located
79 distally from the floodplains of rivers and lakes (Lane and D'Amico, 2016; Lane et al., 2018). Though
80 typically small (Cohen et al., 2016), high biogeochemical processing rates within non-floodplain wetlands
81 have resulted in these systems being termed bioreactors (Marton et al., 2015). Indeed, a literature review
82 of over 600 articles found that the highest reactivity rates (pollutant mass removal per unit time) were
83 found in the smallest water bodies and wetlands (Cheng and Basu, 2017). Further, the high reactivity of
84 individual non-floodplain wetlands can cumulatively improve downgradient water quality conditions
85 (Golden et al., 2019; Evenson et al., 2021). Non-floodplain wetlands may therefore have an outsized
86 impact on a watershed's water quality.

87

88 Non-floodplain wetlands are also important ecosystems affecting water quantity (i.e., for storing and
89 gradually releasing water to downgradient rivers and streams). Specifically, precipitation is captured and
90 stored in non-floodplain wetlands prior to being discharged downgradient. During this storage period,
91 water can infiltrate to recharge aquifers, evaporate or transpire, or eventually “spill” overland and be
92 transported downstream (Jones et al., 2018; Buttle, 2018). These non-floodplain wetland water storage
93 functions attenuate storm flows (Shaw et al., 2012; Fossey and Rousseau, 2016; Blanchette et al., 2022)
94 and recharge groundwaters (Bam et al., 2020), thereby mitigating flood-hazards (Mclaughlin et al., 2014)
95 and ameliorating drought conditions by maintaining baseflow (Ameli and Creed, 2019).

96

97 Despite the important functions provided by non-floodplain wetlands (Biggs et al., 2017; Chen et al.,
98 2022) a substantive data gap remains: no global maps or datasets exist identifying the geospatial location
99 of non-floodplain wetlands and open waters. Regionally focused efforts, such as the recent work by Lane
100 and D'Amico (2016) and Lane et al. (2022) mapped the extent of non-floodplain wetlands (also known as
101 geographically isolated wetlands, Leibowitz, 2015; Mushet et al., 2015) across the geospatially data-rich
102 conterminous United States (CONUS, see abbreviation list in Appendix A). They found that 16-23 % of

103 freshwater systems were potential non-floodplain wetlands, suggesting a substantial yet hitherto unknown
104 portion of the globe's wetlands are likely also this vulnerable water resource.

105
106 Fortunately, geospatial data for identifying aquatic systems, including wetlands, are burgeoning. Global
107 land cover and land use geospatial datasets that include a wetland cover class continue to propagate (Hu
108 et al., 2017a), taking advantage of both lengthy time-series Landsat data (Homer et al., 2020) as well as
109 recently launched advanced high-resolution and/or synthetic aperture radar (SAR) equipped satellites
110 (e.g., Sentinel-1, Sentinel-2, plus many commercially available platforms; Martinis et al., 2022) and
111 topographic data sources and analyses (e.g., Wu et al., 2019b). Examples include the GlobeLand30 (Chen
112 et al., 2015), the European Space Agency (ESA) WorldCover 2020 (ESA, 2020), the Dynamic World
113 (Brown et al., 2022), as well as consortiums focusing on annual land cover change mapping (e.g.,
114 Tsendbazar et al., 2021). Several recent publications review the available wetland-focused datasets,
115 including Hu et al. (2017a, their Table 1), Davidson et al. (2018, their Table S1), Tootchi et al. (2019,
116 their Table 1), and Zhang et al. (2023, their Table 1). We summarize additional emerging global land
117 cover data sets related to surface water and wetlands in Appendix Table B1.

118
119 Lehner and Döll (2004) were amongst the first to publish a geospatially explicit global map focusing on
120 wetland extents. Their Global Lakes and Wetlands Database provides 1 km estimates of wetland
121 abundance. More recent and/or higher resolution wetland-focused datasets have emerged, including the 1
122 km global dataset from Hu et al. (2017b) that incorporates precipitation and a topographic wetness index,
123 and the multi-sourced 500 m composite maps of regularly flooded and groundwater-driven wetlands by
124 Tootchi et al. (2019). Tootchi et al.'s (2019) approach identified small and scattered wetlands. However,
125 they recognized the limitations inherent in their global product (ca. 500 m per pixel resolution) resulted in
126 omission errors for many wetland systems, especially those smaller than their 500 x 500 m (25 ha) data
127 resolution. This suggests, and Tootchi et al. (2019) acknowledged, that many (non-floodplain) wetlands
128 were omitted in the Tootchi et al. (2019) 500 m global product. Cohen et al. (2016) determined non-

129 floodplain wetlands in the CONUS are “unambiguously small”, e.g., their average non-floodplain wetland
130 area was just over two hectares (2.1 ha). Based on the “all or nothing” methodological approach in
131 Tootchi et al. (2019), > 12.5 ha of a given 25.0 ha cell [one homogenous pixel] would have to be
132 identified as wetland in their resampling of the finer-scale data – much larger than the average 2.1 ha
133 wetlands found in Cohen et al. (2016).

134
135 Concurrent with increasingly available global land cover and wetland data, there is an increasing global
136 focus on deriving floodplain and flood hazard-prone areal extents within river networks based on high-
137 resolution topographic data coupled with hydrologic and/or hydraulic modeling (Tullos, 2018;
138 Kundzewicz et al., 2018). The past decade has seen development of multiple regional to continental flood
139 models that span physically based approaches (e.g., 1-,2-, and 3-D hydrodynamic models) to empirical
140 models (including machine-learning approaches and statistical models) (see review by Mudashiru et al.
141 2021). On the global scale, openly accessible global flood models include those reviewed by Hoch and
142 Trigg (2019), namely CaMa-Flood (Yamazaki et al. 2011), GLOFRIS (Winsemius et al. 2013), JRC
143 (Dottori et al. 2016), CIMA-UNEP (Rudari et al. 2015), Fathom (Sampson et al. 2015), and ECMWF
144 (Papperberger et al. 2012). For instance, Sampson et al. (2015) created a global 90 m map of flood-prone
145 areas between 60° N and 56° S using a regional flood-frequency model. More recently, Nardi et al. (2019)
146 published a global floodplain dataset at 250 m resolution that extended from 60° N to 60° S developed
147 through a geomorphic or terrain-based analyses of floodplain elevations and maximum flood-prone areas
148 using a drainage-area scaling variable (Rajib et al. 2021). The evolution of the MERIT Hydro 90 m global
149 hydrography dataset by Yamazaki et al. (2019) and machine-learning approaches (e.g., Zhao et al. 2021)
150 has created additional opportunities to further advance the derivation of global floodplains, with improved
151 identification of flow accumulation area, river-basin shape, and river channel location.

152
153 These wetland-location and floodplain-extent data are critical for watershed-scale sustainable aquatic
154 resource policy decisions (Creed et al., 2017; Golden et al., 2017). The lack of these data can result in

155 disproportionately large model errors and potentially misguided management decisions when non-
156 floodplain wetlands are not incorporated in hydrological and biogeochemical models, ignoring their
157 watershed-scale impacts on flooding, drought, and water quality (Evenson et al., 2018a; Rajib et al., 2020;
158 Golden et al., 2021).

159

160 Here, we provide the first global geospatial dataset of non-floodplain wetlands. We incorporate the recent
161 development of a high-resolution global floodplain mapping algorithm based on digital terrain models by
162 Nardi et al. (2019). We couple these spatial floodplain data with higher-resolution modifications to the
163 gridded global wetland and open water data layers developed by Tootchi et al. (2019) that incorporate the
164 Pekel et al. (2016) satellite-based inundation product, modeled groundwater-driven wetland extent (Fan et
165 al. (2013), and ancillary satellite landcover data from Herold et al. (2015). We test the applicability of our
166 global dataset of non-floodplain wetlands in 21 large and spatial-data rich watersheds spanning nearly
167 700,000 km² across the CONUS. This novel global product identifying non-floodplain wetlands provides
168 for the quantification and estimation of the locations and extent of important aquatic systems with
169 abundant hydrological, biogeochemical, and biological functions, filling a noted research gap while
170 delivering useful data for informed natural resource decision-making and management (Creed et al.,
171 2017; Lane et al., 2022).

172

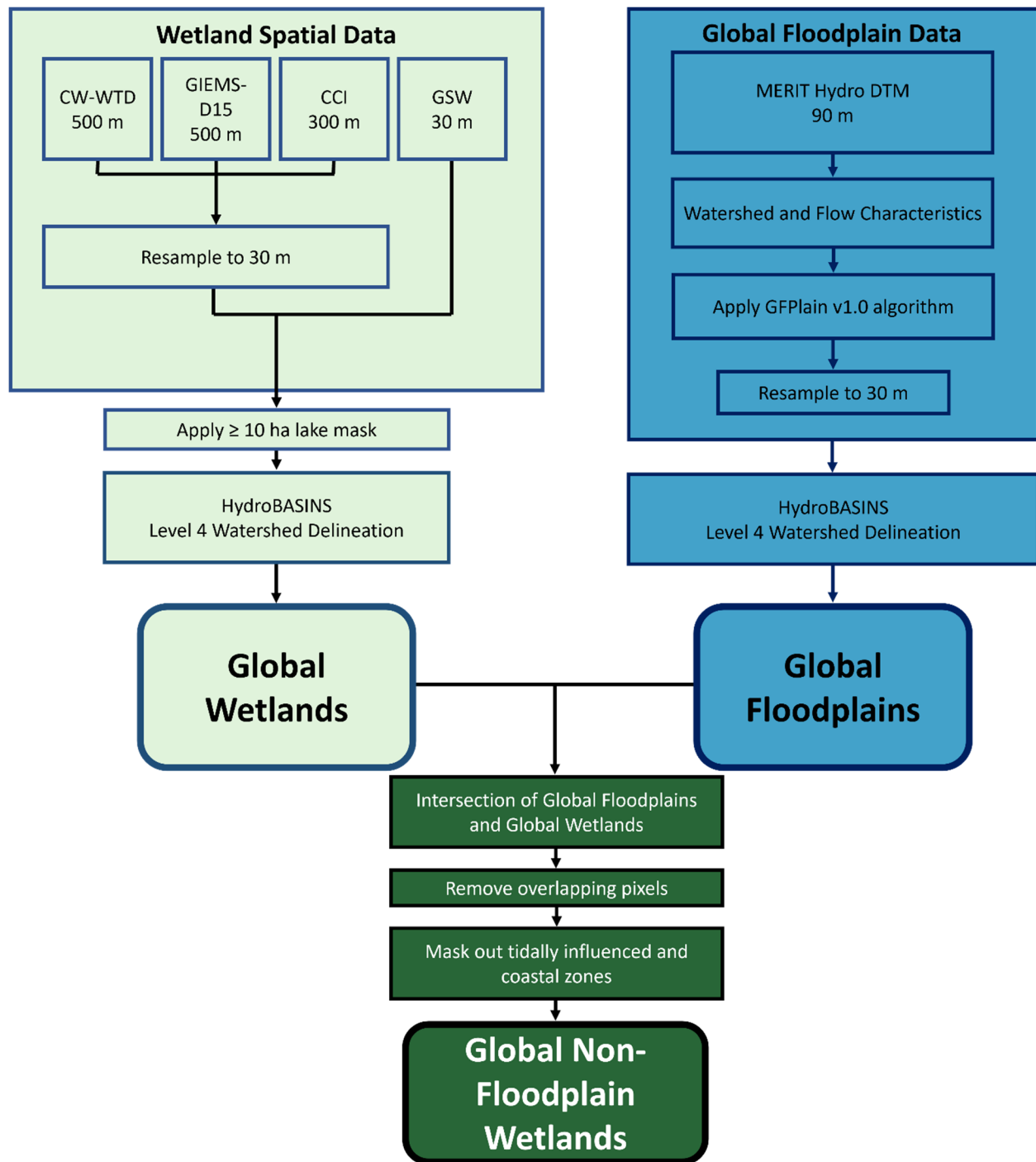
173 **2 Methodology and data**

174

175 Identifying global non-floodplain wetlands required the following steps: 1) determination of global
176 floodplain extent, 2) identification of the global distribution of wetlands, 3) spatial overlay (masking) of
177 floodplains and wetlands to derive a non-floodplain wetland data layer, and 4) data verification and
178 accuracy assessment. Steps 1-3 are outlined in a flow chart given in Fig. 1.

179

180



181
 182 **Figure 1.** Data flow chart identifying the main data sets and processes involved in deriving the Global Floodplain
 183 and Global Wetland data layers, as well as the intersection of those data to create the Global Non-floodplain
 184 Wetlands data product. Curved boxes represent final products, and abbreviations may be found in the text and
 185 Appendix A.

186 2.1 Global floodplain data

187

188 Nardi et al. (2019) combined space-borne elevation data and terrain analysis with a novel open-source
189 algorithm to delineate the geomorphic floodplains across the globe between 60° N and 60° S latitudes.
190 Conceptually, Nardi et al. (2019) identified floodplains from surrounding hillslopes as those low-lying
191 landscape features that have been naturally shaped by accumulated geomorphic effects of past flood
192 events. The original Nardi et al. (2019) dataset was limited in its spatial extent (60° N-60° S) and
193 resolution (250 m); this study sought to delineate global floodplain extent while concurrently identifying
194 floodplain features further up the river network than possible with 250 m pixels. Hence, we utilized the
195 freely available Nardi et al. (2019) GFPlain v1.0 algorithm and coupled this with the MERIT Hydro
196 (Multi-Error Removed Improved Terrain, Yamazaki et al., 2019), global raster digital terrain model data
197 to develop a higher resolution (90 m) geomorphic riverine floodplain for the globe, termed hereafter
198 GFPlain90.

199

200 The development of GFPlain90 required multiple steps. We first extracted elevation data from MERIT
201 Hydro and reprojected the data in UTM zones to prevent distortion when using the GFPlain algorithm.
202 We then developed the drainage network, drainage area, flow accumulation and flow direction data from
203 these data using the established scaling parameters in Nardi et al. (2019; power-law coefficient (a) of 0.01
204 and dimensionless exponent (b) = 0.30). We established 20 km² as the minimum contributing-area
205 threshold required to create the drainage network, balancing the development of a global stream-network
206 distribution and extent with computational requirements. We then globally organized the data by
207 HydroBASINS Level 4 basins (Lehner and Grill, 2013). HydroBASINS provides seamless watershed
208 boundaries and subbasin delineations at global scales; there are 1,342 Level 4 HydroBASINS globally.
209 The floodplain extent resolution of GFPlain90 was resampled (using nearest neighbor) to 30 m for
210 subsequent performance assessment and overlap analyses with the wetland spatial data. All spatial

211 analyses in this study were conducted using ArcGIS Pro v.2.9.x (ESRI, Redlands, California) and GRASS
212 GIS v 7.4.4 (OSGEO, Beaverton, Oregon).

213

214 **2.2 Global Wetland data**

215

216 Tootchi et al. (2019) developed a widely used composite global wetland map at ~500 m by combining
217 multiple data sources, including both satellite-based surface-water inundation mapping and vegetation
218 classification coupled with model-based approaches capturing important groundwater-driven wetland
219 systems. We specifically used the Tootchi et al. (2019) composite map consisting of both regularly
220 surface-water flooded wetlands (“regularly flooded wetlands,” RFWs) and groundwater discharge-
221 maintained wetlands (“groundwater-driven wetlands,” GDWs) as the foundation for our global wetland
222 map. Tootchi et al. (2019) merged the RFW and GDW maps, described below, to form a union product
223 used here that demonstrated a high correlation with available evaluation data, called the composite
224 wetland-water table depth (or CW-WTD).

225

226 **2.2.1 Original composite wetland data**

227

228 Regularly flooded wetlands (RFWs) derived by Tootchi et al. (2019) were based on three data sources: 30
229 m resolution Global Surface Water (GSW) by Pekel et al. (2016), 300 m Climate Change Initiative (CCI)
230 land cover data by Herold et al. (2015), and 500 m GIEMS-D15 wetland extent data by Fluet-Chouinard
231 et al. (2015). GSW data used by Tootchi et al. (2019) were developed from Landsat satellite imagery
232 analyses of pixels identified as inundated at least once during the 32-year period of record by Pekel et al.
233 (2016). CCI input wetland data for Tootchi et al. (2019) included both inundated and wetland vegetation-
234 classed pixels assessed during the period 2008-2012 by Herold et al. (2015). For GIEMS-D15, data
235 included were the mean annual maximum extent of pixels identified as wetlands using multi-sensor
236 satellite data by Prigent et al. (2007), downscaled to ~500 m resolution by Fluet-Chouinard et al. (2015).

237 GSW and CCI input data were resampled to ~500 m resolution using an “all or nothing” approach by
238 Tootchi et al. (2019). This means that a pixel categorization of “wetland” at 500 m resolution was given
239 by Tootchi et al. (2019) only if the majority of resampled finer-resolution input pixels were classed as
240 wetlands. The upward resampling from 30 m and 300 m to 500 m resulted in a loss of informative spatial
241 data on wetland extent from GSW and CCI. Tootchi et al. (2019) calculated that RFWs cover
242 approximately 9.7 % of the global land area (excluding lakes [sourced from (Messenger et al., 2016)],
243 Antarctica, and the Greenland ice sheet).

244

245 Groundwater-driven wetlands (GDWs in the analysis of Tootchi et al., 2019) used in this study were
246 based on the water-table depth estimates by Fan et al. (2013). Fan et al. (2013) developed a 1 km
247 resolution groundwater map based on climate and terrain variables that was validated by over 1 million
248 government-recorded and published observations. Fan et al. (2013) estimated that shallow groundwater
249 influenced nearly 15 % of groundwater-fed surface features, explaining important wetland patterning at
250 global scales (as well as vegetation classes at local and regional scales). A water-table depth threshold of
251 ≤ 20 cm was used by Tootchi et al. (2019) to identify groundwater-driven wetlands and they resampled
252 these data to ~500 m cell resolution. The GDW distribution based on water table depths covered
253 approximately 15 % of the global land mass (including large portions of the Amazon basin, coastal zones,
254 and North American and Siberian peatlands).

255

256 Tootchi et al. (2019) created a merged “final” product, called the composite wetland-water table depth
257 (CW-WTD) map, which is based on the union of the RFW and GDW maps. They measured an
258 approximately 3.8 % overlap between the total land pixels identified as wetlands in both the RFW and
259 GDW maps that comprise the CW-WTD, suggesting the different input maps capture different wetland
260 types. At the global scale, Tootchi et al. (2019) reported spatial Pearson correlations between CW-WTD
261 (wetland fractions at 3 arcmin, or ~4.9 km grids) and wetlands within GLWD (Lehner and Döll, 2004)

262 and Hu et al. (2017b) as $r=0.34$ and $r=0.43$, respectively. Tootchi et al. (2019, their Table 5 and S1)
263 provided additional analysis of the correlations between their global wetland product and existing
264 benchmark data. The total CW-WTD global wetland estimate was $\sim 21.1\%$ of the land mass, or
265 approximately 27.5 million km^2 (excluding large lakes, Antarctica, and the Greenland ice sheet; Tootchi
266 et al., 2019).

267

268 **2.2.2 Derived global wetland data**

269

270 To account for the acknowledged limitations of the Tootchi et al. (2019) data and to accurately identify
271 more of the existing small and, specifically, non-floodplain wetlands across the globe (e.g., those <25 ha),
272 we improved upon and augmented the CW-WTD (Tootchi et al., 2019) global wetland data layer with the
273 30 m native-resolution GSW (Pekel et al., 2016) and 300 m native-resolution CCI (Herold et al., 2015)
274 data. The inclusive wetland categories of Tootchi et al. (2019) were maintained, namely at least one
275 inundation event over a 32 year range (for GSW data) and CCI pixels defined as "...mixed classes of
276 flooded areas with tree covers, shrubs, or herbaceous covers plus inland water bodies..." (Tootchi et al.,
277 2019, p. 193). However, for our analysis we resampled the 500 m CW-WTD product to 30 m using the
278 nearest-neighbor approach and then added any identified wetland pixel from the CCI data (resampled
279 from 300 m to 30 m) and inundated pixel from the GSW data (30 m resolution). Resampling to a finer
280 resolution (as we did in our analysis) does not result in data losses: the same data are retained but are
281 divided into equal, smaller parts. However, moving from a finer resolution to coarser resolution (as in the
282 CW-WTD dataset's "all-or-nothing" approach) does cause data losses: fine-scale data are necessarily
283 aggregated (often by averaging) to a larger grid cell size, and therefore less information is retained. To
284 compensate for this data loss in the CW-WTD dataset, the finer resolution GSW (30 m) and CCI (300 m)
285 data were added back into the dataset. This resulted in a novel and encompassing wetland ensemble end-
286 product, hereafter termed the Global Wetlands dataset. This new dataset is inclusive of both finer-

287 resolution (30 m and 300 m) data, thereby accounting for a wide range of wetland sizes – such as smaller
288 non-floodplain wetlands (Cohen et al., 2016) – that remained unmapped by Tootchi et al. (2019).

289

290 **2.3 Global Non-Floodplain Wetlands (Global NFWs)**

291

292 To identify non-floodplain wetlands specifically, we overlaid our GFPlain90 floodplain data with our
293 mapped Global Wetlands data to mask wetland pixels collocated on the floodplain. Then, to avoid tidally
294 influenced wetlands, we conducted a region-group analysis to identify connected pixels abutting coastal
295 shorelines in order to mask wetlands in coastal areas (e.g., those directly abutting the shoreline and
296 spatially connected to tidally influenced areas). We used a four-directional contagion criterion to identify
297 connected pixels (i.e., those connected in cardinal directions). Subsequently, we applied a 1 km buffer to
298 the HydroBASINS (Lehner and Grill, 2013) coastline area and removed from our analyses any wetland
299 region-group partially or completely overlain by the 1 km coastline buffer. In addition, Tootchi et al.
300 (2019) removed lake systems (≥ 10 ha) from their wetland-focused data by masking aquatic layers using
301 HydroLAKES (Messenger et al., 2016). To avoid including large lakes in our emerging non-floodplain
302 wetland geospatial data, we also applied the HydroLAKES mask and removed lake systems ≥ 10 ha
303 (Messenger et al., 2016) from our Global Wetlands dataset. Thus, our final global non-floodplain wetland
304 data product (hereafter Global NFWs) did not include fluvial floodplain wetlands nor coastal wetland
305 complexes and large open water lacustrine (lake-like, Cowardin et al., 1979) systems.

306

307 **2.4 Data verification and assessment**

308

309 We evaluated the global products developed here through comparison of high-resolution floodplain and
310 wetland extent data from 21 basins representing disparate climatic (according to the Köppen-Geiger
311 classification, Beck et al., 2018), elevation, and land-use gradients within the CONUS (Fig. 2;

312 summarized in Table B2). We specifically focused on the CONUS for product assessment because of its
313 wide-ranging data availability and diversity of physiographic and climatic regions.

314

315 **2.4.1 Verifying floodplain extent**

316

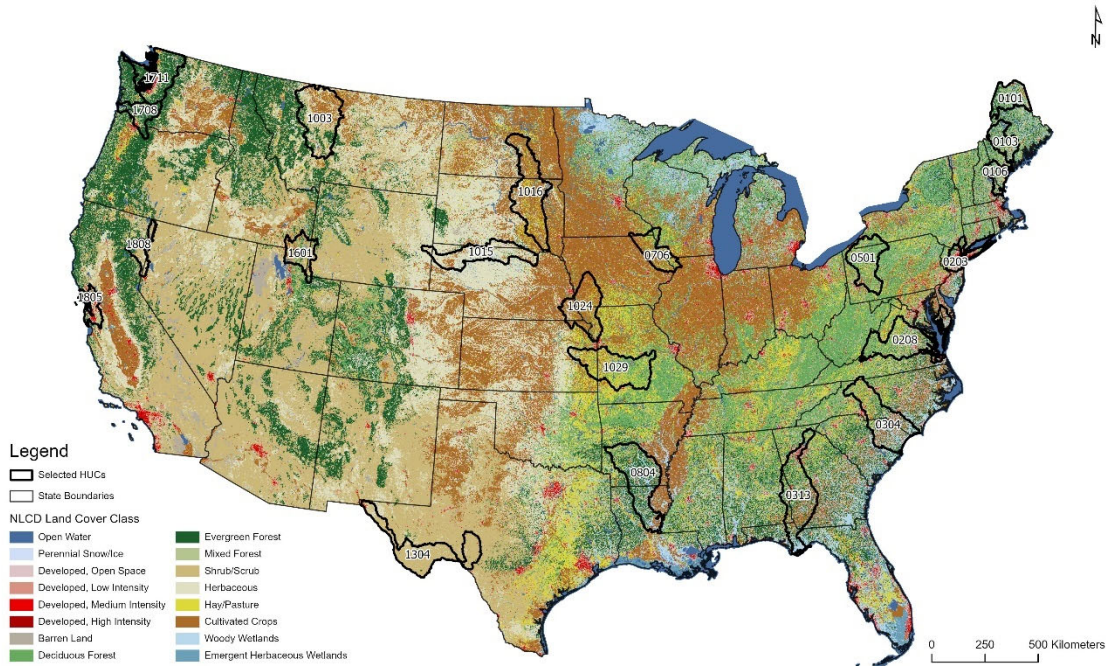
317 We used a recently developed machine learning (ML)-based 30 m resolution CONUS floodplain dataset
318 (Woznicki et al., 2019) as the benchmark to evaluate our GFPlain90 global floodplain data. Specifically,
319 the ML model by Woznicki et al. (2019) used the U.S. Federal Emergency Management Agency (FEMA)
320 100 yr floodplain (i.e., a 1 % chance of coastal or fluvial flood-inundation in a given year; Jakubínský et
321 al., 2021) as the training data, and subsequently used soil and topographic characteristic along with land
322 cover to identify potential floodplain grid cells across CONUS at 30 m resolution. Woznicki et al. (2019)
323 reported that their ML approach correctly identified ~79 % of the FEMA 100 yr coastal and fluvial
324 floodplains, providing spatially complete 100 yr floodplain coverage totaling 980,450 km² across the
325 CONUS.

326

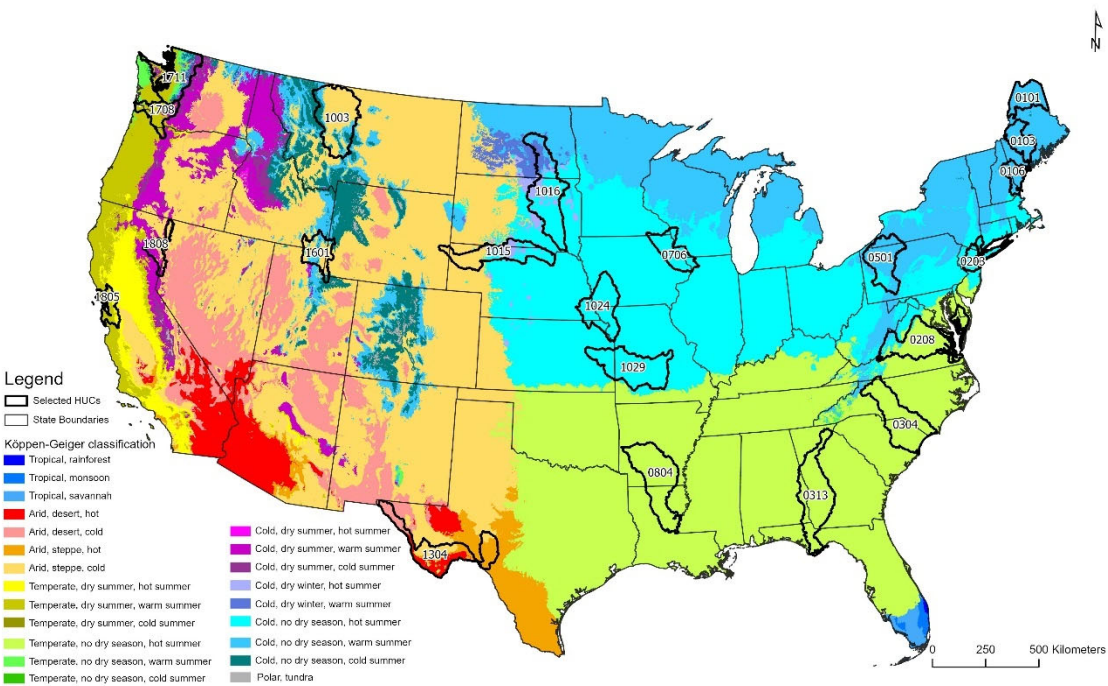
327 **2.4.2 Verifying wetland and non-floodplain wetland extent**

328

329 We evaluated our inclusive Global Wetlands and Global NFWs datasets in 21 basins covering ~680,000
330 km² (Fig. 2). We contrasted our products to the 2016 National Land Cover Database (NLCD, Dewitz,
331 2019). The NLCD is a 30 m Landsat satellite-based geospatial product with an overall accuracy of 86 %
332 that incorporates high-resolution aerial imagery of wetland location for model parameterization and
333 calibration (Jin et al., 2019; Wickham et al., 2021). Three NLCD classes were selected for comparison
334 with the Global Wetland product: woody wetlands, emergent herbaceous wetlands, and open water. To



335



336

337 **Figure 2.** Twenty-one validation watersheds were selected from across CONUS to capture the breadth and extent of
 338 land use (top, NLCD 2019) and climate and physiographic regions (bottom) within CONUS according to the
 339 Köppen-Geiger classification (Beck et al., 2018); also summarized in Table B2). The Hydrologic Unit Code (HUC)
 340 classifications are sourced from USGS Watershed Boundary Dataset (2022).

341
 342 assess the relative improvement of our 30 m Global Wetlands and Global NFWs dataset with the 500 m
 343 Tootchi et al. (2019) data, we also contrasted the CW-WTD with the NLCD classes within the
 344 verification watersheds. For equal comparisons, following Tootchi et al. (2019) we used the Messenger et
 345 al. (2016) HydroLAKES to mask out large lake systems (≥ 10 ha) from both the Global Wetlands and the
 346 NLCD data within the 21 verification watersheds.

347

348 **2.4.3 Standard performance measures**

349

350 We evaluated the floodplain and wetland spatial data within the 21 validation watersheds using
 351 commonly employed performance measures. Following Wing et al. (2017), we first created a contingency
 352 table for our performance assessment (Table 1). As noted, we selected 20 km² as the minimum
 353 contributing area to develop stream networks in our global floodplain analysis, a reasonable area for flow-
 354 accumulation that balances computational efficiency for global geospatial model development. Woznicki
 355 et al. (2019), our benchmark floodplain dataset, used a 4.5 km² contributing area in their high-resolution
 356

357 **Table 1.** Contingency table of possible outcomes for each cell used in assessing the performance of either the
 358 floodplain or wetland geospatially modeled data. We contrasted published benchmark data from Woznicki et al.
 359 (2019) for floodplain extent against modeled GFPlain90 data. Wetland comparisons contrasted NLCD wetlands
 360 (Dewitz, 2019, open water and wetland classes) against both Global Wetlands and Global NFWs data. Table is
 361 modified from Wing et al. (2017). The subscript “1” equates to a positive outcome or overlapping extent for either
 362 the modeled (M) or benchmark (B) data whereas a zero means no data overlap or a negative outcome.

	Floodplain [or Wetland] in Benchmark data	Not Floodplain [or Wetland] in Benchmark data
Floodplain [or Wetland] in Modeled data	M ₁ B ₁	M ₁ B ₀
Not Floodplain [or Wetland] in Modeled data	M ₀ B ₁	M ₀ B ₀

363

364 CONUS analysis. To appropriately compare between datasets of two varying resolutions, we removed
365 stream and river network components from the Woznicki et al. (2019) validation dataset developed with
366 contributing areas $<20 \text{ km}^2$, as our model did not discern landscape data at that granularity.

367
368 To provide a full assessment of our geospatial modeling performance, we contrasted our GFPlain90
369 floodplain dataset across the 21 validation watersheds using the approaches described below following
370 Sampson et al. (2015), Wing et al. (2017), and others (e.g., Bates and De Roo, 2000; Alfieri et al., 2014;
371 Sangwan and Merwade, 2015; Jafarzadegan et al., 2018; Woznicki et al., 2019). We first contrasted our
372 GFPlain90 floodplains to Woznicki et al. (2019), our benchmark floodplain data. We then analyzed the
373 watershed-scale comparison of our Global Wetlands product versus the NLCD wetlands (combined open
374 water and wetland classes), our benchmark wetlands data. We followed with a comparison focusing only
375 on our Global NFWs data and those NLCD wetlands and open water pixels that were determined to be
376 non-floodplain systems (i.e., NLCD data that also do not overlap the GFPlain90 data nor coastal waters
377 and with lakes $>10 \text{ ha}$ removed). These NLCD wetlands were our benchmark non-floodplain wetland
378 data. Lastly, we assessed the mean and aggregate error bias of our analyses by exploring results at coarser
379 spatial granularity (i.e., 1 km pixel size) along the riverine network (for floodplain assessment) and, for
380 wetland metrics, throughout the entirety of our 21 performance assessment watersheds (Sampson et al.,
381 2015; Wing et al., 2017). The metrics described below and in Table 2 were used in our analyses.

382
383 *Hit Rate* (Bates and De Roo, 2000; Horritt and Bates, 2002; Tayefi et al., 2007) also referred to as Recall
384 (Woznicki et al., 2019) and Correct (Sangwan and Merwade, 2015), measures how well a geospatial
385 model classification replicates the benchmark data but does not penalize for overprediction. *H* varies from
386 0, where there is no overlap between the modeled data and the benchmark data, to 1 where the modeled
387 data completely contain the benchmark data. *Precision* (Woznicki et al., 2019), also known as Spatial
388 Coincidence (Tootchi et al., 2019), indicates the proportion of the benchmark data that are correctly
389 predicted and mapped in the modeled data. This metric, *P*, also ranges from 0 to 1 with higher values

390 **Table 2.** Performance metrics used in validation assessments of floodplain and wetland data layers. Data for
 391 assessment (e.g., M_1B_1) follow that given in Table 1 and modified from Wing et al. (2017), with the exception of
 392 equations 7 and 8 (see text).

Equation Number	Metrics	Equation	Range
1	Hit Rate (H)	$Hit\ Rate\ (H) = \frac{M_1B_1}{M_1B_1 + M_0B_1}$	0 - 1, higher is “better”
2	Precision (P)	$Precision\ (P) = \frac{M_1B_1}{M_1B_1 + M_1B_0}$	0 - 1, higher is “better”
3	False Alarm Ratio (FA)	$False\ Alarm\ Ratio\ (FA) = \frac{M_1B_0}{M_1B_0 + M_1B_1}$	0 - 1, lower is “better”
4	Critical Success Index (CSI)	$Critical\ Success\ Index\ (CSI) = \frac{M_1B_1}{M_1B_1 + M_0B_1 + M_1B_0}$	0 - 1, higher is “better”
5	F1	$F1 = 2 \left(\frac{H \times P}{H + P} \right)$	0 - 1, higher is “better”
6	Error Bias (EB)	$Error\ Bias\ (EB) = \frac{M_1B_0}{M_0B_1}$	0 - ∞; <1 underprediction, 1 = no bias, >1 indicate overprediction
7	Mean Absolute Error (EA)	$Mean\ Absolute\ Error\ (EA) = \frac{\sum_{i=1}^N M-B }{N}$	0 - 1, lower is “better”
8	Aggregate Error Bias (BA)	$Aggregate\ Error\ Bias\ (BA) = \frac{\sum_{i=1}^N M-B}{N}$	-1 to 1, negative values indicate underprediction, positive values overprediction

393
 394 indicating better performance. The *False Alarm Ratio* (Sampson et al., 2015; Wing et al., 2017) also
 395 known as the False Discovery Ratio, quantifies modeled data overprediction relative to the benchmark
 396 data. *F* varies from 0 (zero false alarms) to 1 (all false alarms); lower values are considered better
 397 performance. The False Alarm Ratio can also be calculated as 1 - *Precision* (Woznicki et al., 2019). The
 398 *Critical Success Index* (CSI, Bates and De Roo, 2000; Aronica et al., 2002; Werner et al., 2005; Fewtrell
 399 et al., 2008), also known as Jaccard’s Index (Tootchi et al., 2019), and Fit (Sangwan and Merwade, 2015),
 400 penalizes for both over- and under-prediction, ranging from 0 (no match) to 1 (perfect match). Woznicki
 401 et al. (2019) utilized a performance metric, *F1*, which combines the *Hit Rate* (called Recall by Woznicki
 402 et al. 2019) and *Precision* using their harmonic mean. *F1* also varies from 0 to 1, with higher values
 403 indicating better performance. *Error Bias* (*EB*) characterizes the tendency of the model towards under- or

404 over-prediction (Sampson et al., 2015). Values of 1 indicate no bias, $0 \leq EB < 1$ indicates underprediction
405 whereas $1 < EB \leq \infty$ indicates the model is tending towards overprediction. Lastly, two additional metrics
406 were calculated that assessed performance at the 30 arc-sec (~1 km) scale. These measures, *Mean*
407 *Absolute Error* and *Aggregate Error Bias* (Sampson et al., 2015; Wing et al., 2017), characterize the data
408 accuracy across large spatial extents. Large spatial extents are areas where 30 m data and overlap
409 accuracy is less a concern than general dataset performance for broad-scale end-user applications (e.g.,
410 when coarser, watershed-scale “lumped” hydrologic characterizations of water storage are all that is
411 required). For these metrics, both estimated and benchmark data were resampled to 1 km resolution
412 across the whole of each watershed; values within each 1 km pixel ranged from 0 to 1 and represented the
413 fraction of the 30 m resolution estimates and benchmark data. We assessed floodplain estimates after
414 calculating the fractional abundance comprising each 1 km² pixel within a 1 km buffer around the
415 Woznicki et al. (2019) floodplain data. We additionally analyzed all wetlands at the watershed-scale as
416 well as focusing on non-floodplain wetlands (e.g., wetlands exclusive of the GFPlain90 floodplain or
417 coastal connections, our target aquatic system). In Eq. 7 and 8 (given in Table 2), M is the area estimated
418 as floodplain (or wetland), B is the benchmark floodplain (or wetland) area, and N is the number of 1 km
419 cells with data. *Mean Absolute Error* and *Aggregate Error Bias* were calculated for each of the 21 HUCs,
420 following Wing et al. (2017).

421

422 **3 Results**

423

424 **3.1 Floodplain data performance**

425

426 The GFPlain90 floodplain data (Fig. 3) performed well when contrasted with the 100 yr coastal and
427 fluvial floodplain extent data from Woznicki et al. (2019), even though our analyses do not map coastal
428 floodplains. A median Hit Rate of 0.77 suggests that nearly 80% of the benchmark floodplain from
429 Woznicki et al. (2019) was similarly captured by the GFPlain90 floodplain data (see Appendix Table B3).

430 In addition, the median False Alarm of 0.26 indicates that for every three pixels correctly identified as
431 within the Woznicki et al. (2019) floodplain, one pixel was incorrectly identified as such (i.e., a
432 commission error measure); this is evident in wider GFPlain90 floodplains in lower river reaches than
433 predicted by Woznicki et al. (2019). These performance values are similar to those reported by Woznicki
434 et al. (2019, False Alarm 0.22) and Wing et al. (2017, False Alarm 0.34-0.37). Critical Success Index
435 (CSI) scores penalize for over-prediction; our median value of 0.53 approximates previously published
436 regional (e.g., Sangwan and Merwade, 2015, CSI values ranging from 0.44-0.89) and continental flood-
437 extent approaches (e.g., Sampson et al., 2015, CSI values from 0.43-0.67; Wing et al., 2017; CSI values
438 between 0.50 and 0.55 reported). Median Precision (0.74) and F1 (0.70) values approximate those in the
439 literature as well (e.g., Woznicki et al., 2017 reported values of 0.78 for both). Median Error Bias values
440 of 1.0 suggests the model neither over-estimates nor under-estimates floodplain extents (Wing et al.
441 2017). Mean Absolute Error of 0.08 reported here indicates an approximate 8 % difference between our
442 GFPlain90 model and that of Woznicki et al. (2017) at the 1 km cell resolution.

443

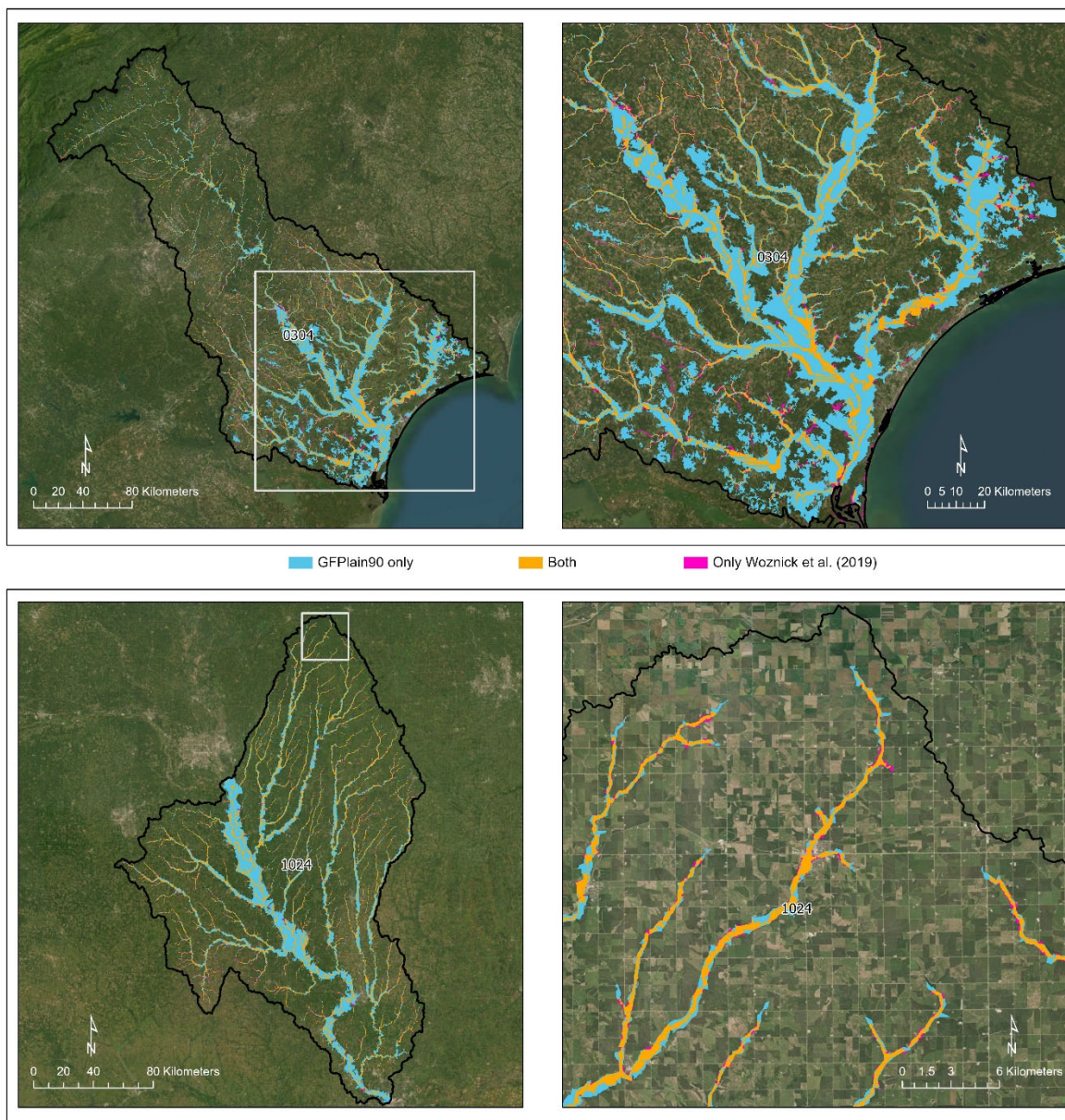
444 **3.2 Wetland data performance**

445

446 **3.2.1 Global Wetland dataset**

447

448 The novel ensemble Global Wetlands approach improved upon the previously published Tootchi et al.
449 (2019) research product, the CW-WTD (Table 3) when contrasted with CONUS data. A median Hit Rate
450 value of 0.24 indicates that both the inclusive Global Wetlands and CW-WTD captured ~one-quarter of
451 the high-resolution, 30-m pixel size NLCD wetlands and open waters in the validation dataset. However,
452 across the 21 validation watersheds the Global Wetlands dataset developed here correctly identified more
453 wetlands than the CW-WTD alone, as indicated by an 8% mean increase in Precision, 43 % increase in
454 Critical Success Index, 38 % increase in F1, a -8 % decrease in the False Alarm ratio, and a 21 %



456

457 **Figure 3.** The robust performance of GFPlain90 relative to the benchmark Woznicki et al. (2019) floodplain data is
 458 evident in the two rows, with the top panels (HUC_0304) a coastal watershed spanning North and South Carolina,
 459 USA, and the bottom two panels different spatial extents of a midwestern USA watershed (HUC_1024). The
 460 mainstem of the river network appeared wider in the GFPlain90 data in both examples, especially in the lower
 461 reaches, though the complete network was well represented (i.e., floodplains were identified to the furthest extent of
 462 the stream network's headwaters). Satellite imagery is sourced from ESRI (2022).

463 decrease in Error Bias. At coarser, 1 km² scales, there was a slight decrease in the Mean Absolute Error
464 associated with the Global Wetlands, and no difference in Aggregate Error Bias between the data
465 products.

466

467 **3.2.2 Global Non-Floodplain Wetland (Global NFW) dataset**

468

469 Non-floodplain wetland identification using the Global Wetlands data (i.e., Global NFWs) similarly
470 improved upon the CW-WTD product (Fig. 4). For instance, though the Hit Rate values were low (e.g.,
471 median values ≤ 0.10), underscoring both the difficulty in mapping non-floodplain wetlands and the
472 challenge of assessing performance using high-resolution data, Global NFW analyses correctly identified
473 50 % more non-floodplain wetlands than the CW-WTD (Table 4, Tootchi et al., 2019). Improvements
474 when focusing on non-floodplain wetlands were found in every category with the Global NFWs dataset,
475 demonstrating increased non-floodplain wetland accuracy versus the original CW-WTD across the
476 median metric values for Precision, Critical Success Index, F1, False Alarms, and Error Bias (e.g., 33 %
477 increase in Precision, 20 % increase in Critical Success Index, 10 % increase in F1 scores, and a 12 %
478 decrease in False Alarms and a 19 % decrease in Error Bias). There was no difference between the
479 datasets with median values for Mean Absolute Error (median values for both = 0.09) or Aggregate Error
480 Bias (median values for both = 0.07). Thus, at the 1 km² cell size, there was <10 % difference between
481 both the CW-WTD and the Global NFWs and the benchmark NLCD non-floodplain wetlands and open
482 waters (with the difference mostly stemming from an increase in identified wetlands with both CW-WTD
483 and Global NFWs, as indicated with the positive Aggregate Error Bias values).

484

485

486

487

488 **Table 3.** Spatial performance assessment of both the Global Wetland (abbreviated here as GW) and CW-WTD
489 (abbreviated here as WTD, Tootchi et al., 2019) datasets when contrasted with the benchmark NLCD wetlands
490 (Dewitz, 2019). The first six equations directly assess the spatial concordance and overlap between each spatial
491 dataset and the benchmark (e.g., CW-WTD contrasted with the NLCD), whereas Mean Absolute Error (MAE, Eq.
492 7) and Aggregate Error Bias (AEB, Eq. 8) are coarser fractional analyses measured throughout each watershed (e.g.,
493 the proportional abundance NLCD within each 1 km² cell is contrasted with the proportional abundance of Global
494 Wetlands predicted correctly within that cell).

Hydrologic Unit Code (HUC) ID	Hit Rate		Precision		False Alarm		Critical Success	
	(Eq. 1)		(Eq. 2)		(Eq. 3)		(Eq. 4)	
	WTD	GW	WTD	GW	WTD	GW	WTD	GW
HUC_0101	0.31	0.32	0.51	0.53	0.49	0.47	0.24	0.25
HUC_0103	0.26	0.28	0.42	0.45	0.58	0.55	0.19	0.21
HUC_0106	0.25	0.27	0.41	0.44	0.59	0.56	0.18	0.20
HUC_0203	0.12	0.12	0.51	0.53	0.49	0.47	0.11	0.11
HUC_0208	0.31	0.33	0.56	0.65	0.44	0.35	0.25	0.28
HUC_0304	0.42	0.43	0.65	0.69	0.35	0.31	0.35	0.36
HUC_0313	0.39	0.41	0.58	0.64	0.42	0.36	0.30	0.33
HUC_0501	0.15	0.17	0.57	0.64	0.43	0.36	0.14	0.15
HUC_0706	0.24	0.25	0.86	0.92	0.14	0.08	0.23	0.24
HUC_0804	0.45	0.46	0.70	0.75	0.30	0.25	0.38	0.40
HUC_1003	0.14	0.16	0.32	0.41	0.68	0.59	0.11	0.13
HUC_1015	0.25	0.40	0.17	0.42	0.83	0.58	0.12	0.26
HUC_1016	0.13	0.16	0.54	0.70	0.46	0.30	0.12	0.15
HUC_1024	0.10	0.10	0.67	0.75	0.33	0.25	0.09	0.10
HUC_1029	0.10	0.13	0.51	0.72	0.49	0.28	0.09	0.13
HUC_1304	0.02	0.02	0.44	0.52	0.56	0.48	0.02	0.02
HUC_1601	0.29	0.33	0.34	0.45	0.66	0.55	0.19	0.24
HUC_1708	0.24	0.24	0.48	0.49	0.52	0.51	0.19	0.20
HUC_1711	0.09	0.10	0.46	0.51	0.54	0.49	0.08	0.09
HUC_1805	0.14	0.15	0.62	0.64	0.38	0.36	0.13	0.13
HUC_1808	0.12	0.13	0.51	0.55	0.49	0.45	0.11	0.11
Median	0.24	0.24	0.51	0.55	0.49	0.45	0.14	0.20
Difference		0.00		0.04		-0.04		0.06
Change (%)		0.0		7.8		-8.2		42.9

495

496 **Table 3.** (Continued)

Hydrologic Unit Code (HUC) ID	F1		Error Bias		MAE		AEB	
	(Eq. 5)		(Eq. 6)		(Eq. 7)		(Eq. 8)	
	WTD	GW	WTD	GW	WTD	GW	WTD	GW
HUC_0101	0.38	0.40	0.43	0.40	0.18	0.17	0.09	0.09
HUC_0103	0.32	0.34	0.50	0.47	0.16	0.15	0.06	0.07
HUC_0106	0.31	0.33	0.49	0.46	0.20	0.19	0.08	0.08
HUC_0203	0.19	0.20	0.13	0.13	0.36	0.36	0.28	0.28
HUC_0208	0.40	0.44	0.35	0.27	0.17	0.17	0.09	0.10
HUC_0304	0.51	0.53	0.39	0.34	0.21	0.21	0.12	0.13
HUC_0313	0.47	0.50	0.48	0.38	0.16	0.16	0.07	0.09
HUC_0501	0.24	0.26	0.14	0.11	0.10	0.10	0.09	0.09
HUC_0706	0.37	0.39	0.05	0.03	0.12	0.12	0.11	0.12
HUC_0804	0.55	0.57	0.36	0.29	0.20	0.20	0.12	0.14
HUC_1003	0.19	0.23	0.34	0.27	0.04	0.04	0.02	0.02
HUC_1015	0.21	0.41	1.59	0.91	0.05	0.04	-0.01	0.00
HUC_1016	0.21	0.26	0.13	0.08	0.26	0.26	0.23	0.24
HUC_1024	0.17	0.18	0.05	0.04	0.14	0.14	0.13	0.14
HUC_1029	0.17	0.22	0.11	0.06	0.11	0.12	0.10	0.11
HUC_1304	0.04	0.04	0.02	0.02	0.08	0.08	0.08	0.08
HUC_1601	0.31	0.38	0.80	0.59	0.05	0.05	0.01	0.01
HUC_1708	0.32	0.33	0.34	0.33	0.15	0.15	0.08	0.08
HUC_1711	0.15	0.17	0.12	0.11	0.17	0.17	0.14	0.15
HUC_1805	0.23	0.24	0.10	0.10	0.25	0.26	0.21	0.21
HUC_1808	0.20	0.20	0.13	0.12	0.09	0.09	0.07	0.07
Median	0.24	0.33	0.34	0.27	0.16	0.15	0.09	0.09
Difference		0.09		0.07		-0.01		0.00
Change (%)		37.5		-20.6		-6.3		0.0

497

498

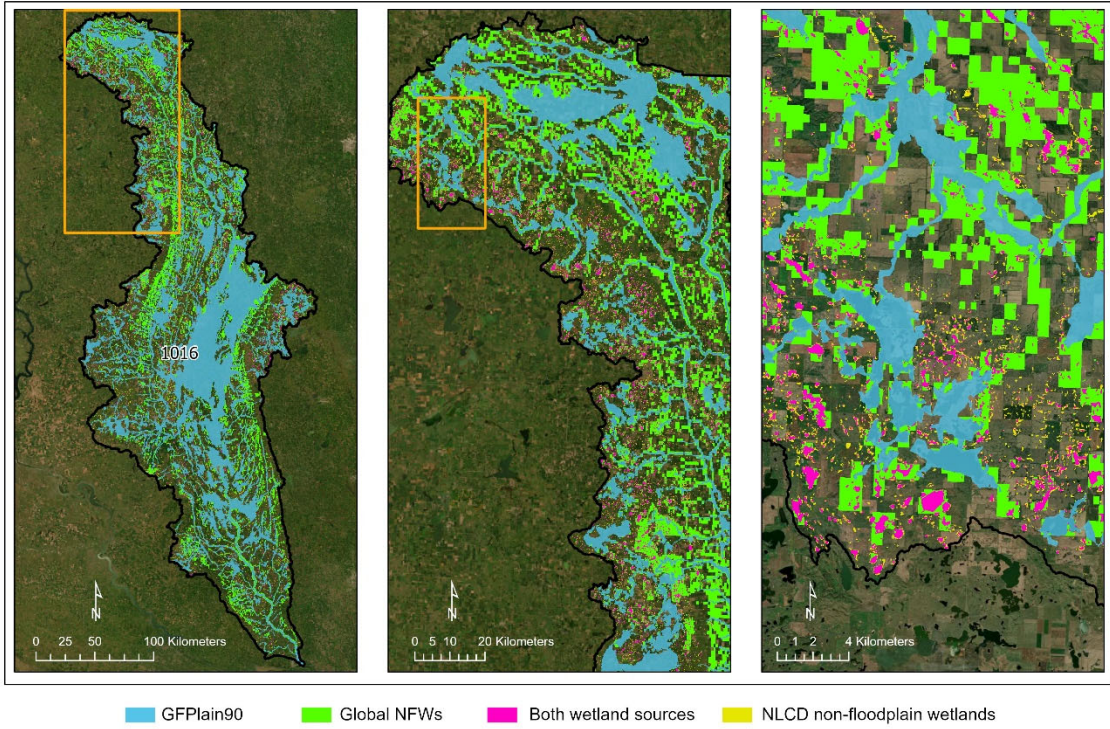


Figure 4. Demonstration of the relative accuracy of the Global NFWs in identifying non-floodplain wetlands using a Prairie Pothole Region watershed (HUC_1016, see Fig. 2) replete with abundant non-floodplain wetlands. Correctly identified wetlands occur in both wetland sources (magenta color). Omission errors (NLCD non-floodplain wetlands, smaller systems in yellow) and commission errors (Global NFWs, green) are evident as a result of the higher resolution of the NLCD validation dataset. Satellite imagery sourced from ESRI (2022). Note the scale increasing from left panel to right panel (i.e., the orange box in the first panel is shown in the second panel at a higher resolution, and the box in the second panel is shown in the last panel at an even higher resolution).

507 **Table 4.** Non-floodplain wetland performance metrics contrasting both the Global NFWs (abbreviated here as
508 GNFW) and CW-WTD (abbreviated here as WTD, Tootchi et al., 2019) non-floodplain wetland spatial data with the
509 benchmark NLCD wetlands (Dewitz, 2019). Descriptions of the metrics are the same as in Table 3, though the focus
510 here is on wetlands outside the GFPlain90-derived floodplain.

Hydrologic Unit Code (HUC) ID	Hit Rate		Precision		False Alarm		Critical Success Index	
	(Eq. 1)		(Eq. 2)		(Eq. 3)		(Eq. 4)	
	WTD	GNFW	WTD	GNFW	WTD	GNFW	WTD	GNFW
HUC_0101	0.24	0.25	0.43	0.45	0.57	0.55	0.18	0.19
HUC_0103	0.17	0.18	0.30	0.32	0.70	0.68	0.12	0.13
HUC_0106	0.15	0.18	0.14	0.17	0.86	0.83	0.08	0.10
HUC_0203	0.12	0.13	0.20	0.23	0.80	0.77	0.08	0.09
HUC_0208	0.14	0.16	0.34	0.41	0.66	0.59	0.11	0.13
HUC_0304	0.26	0.28	0.45	0.49	0.55	0.51	0.20	0.21
HUC_0313	0.21	0.23	0.35	0.40	0.65	0.60	0.15	0.17
HUC_0501	0.05	0.07	0.32	0.41	0.68	0.59	0.05	0.06
HUC_0706	0.05	0.06	0.63	0.72	0.37	0.28	0.05	0.05
HUC_0804	0.30	0.31	0.51	0.55	0.49	0.45	0.23	0.25
HUC_1003	0.04	0.07	0.13	0.21	0.87	0.79	0.03	0.05
HUC_1015	0.07	0.25	0.05	0.28	0.95	0.72	0.03	0.15
HUC_1016	0.07	0.11	0.31	0.53	0.69	0.47	0.06	0.10
HUC_1024	0.02	0.04	0.18	0.41	0.82	0.59	0.02	0.04
HUC_1029	0.03	0.06	0.25	0.58	0.75	0.42	0.03	0.06
HUC_1304	0.00	0.00	0.26	0.33	0.74	0.67	0.00	0.00
HUC_1601	0.05	0.09	0.07	0.16	0.93	0.84	0.03	0.06
HUC_1708	0.06	0.06	0.33	0.35	0.67	0.65	0.05	0.05
HUC_1711	0.04	0.05	0.22	0.27	0.78	0.73	0.04	0.05
HUC_1805	0.06	0.07	0.27	0.30	0.73	0.70	0.05	0.06
HUC_1808	0.05	0.06	0.25	0.36	0.75	0.64	0.04	0.06
Median	0.06	0.09	0.27	0.36	0.73	0.64	0.05	0.06
Difference		0.03		0.09		-0.09		0.01
Change (%)		50.0		33.3		-12.3		20.0

511

512

513 **Table 4.** (Continued)

Hydrologic Unit Code (HUC) ID	F1		Error Bias		Mean Absolute Error		Aggregate Error Bias	
	(Eq. 5)		(Eq. 6)		(Eq. 7)		(Eq. 8)	
	WTD	GFW	WTD	GFW	WTD	GFW	WTD	GFW
HUC_0101	0.31	0.32	0.41	0.39	0.16	0.16	0.08	0.09
HUC_0103	0.21	0.23	0.48	0.46	0.14	0.14	0.06	0.06
HUC_0106	0.14	0.18	1.11	1.03	0.11	0.11	-0.01	0.00
HUC_0203	0.15	0.17	0.53	0.51	0.09	0.09	0.03	0.03
HUC_0208	0.20	0.23	0.32	0.28	0.10	0.10	0.07	0.07
HUC_0304	0.33	0.35	0.44	0.40	0.17	0.17	0.08	0.09
HUC_0313	0.27	0.29	0.51	0.45	0.12	0.12	0.05	0.06
HUC_0501	0.09	0.11	0.12	0.10	0.09	0.09	0.07	0.08
HUC_0706	0.09	0.10	0.03	0.02	0.09	0.09	0.09	0.09
HUC_0804	0.38	0.40	0.43	0.37	0.13	0.13	0.07	0.07
HUC_1003	0.07	0.10	0.32	0.26	0.02	0.03	0.01	0.01
HUC_1015	0.06	0.26	1.46	0.85	0.03	0.02	-0.01	0.00
HUC_1016	0.11	0.19	0.17	0.11	0.15	0.15	0.12	0.13
HUC_1024	0.03	0.07	0.09	0.06	0.05	0.05	0.04	0.05
HUC_1029	0.05	0.11	0.09	0.05	0.08	0.08	0.07	0.07
HUC_1304	0.00	0.01	0.01	0.01	0.06	0.06	0.05	0.06
HUC_1601	0.05	0.11	0.68	0.50	0.02	0.02	0.00	0.01
HUC_1708	0.10	0.10	0.12	0.12	0.11	0.11	0.09	0.10
HUC_1711	0.07	0.09	0.16	0.15	0.09	0.09	0.07	0.07
HUC_1805	0.10	0.11	0.18	0.17	0.10	0.10	0.07	0.07
HUC_1808	0.08	0.11	0.15	0.12	0.02	0.02	0.01	0.01
Median	0.10	0.11	0.32	0.26	0.09	0.09	0.07	0.07
Difference		0.01		-0.06		0.00		0.00
Change (%)		10.0		-18.8		0.0		0.0

514

515

516 **3.3 Global extent analyses and synthesis**

517

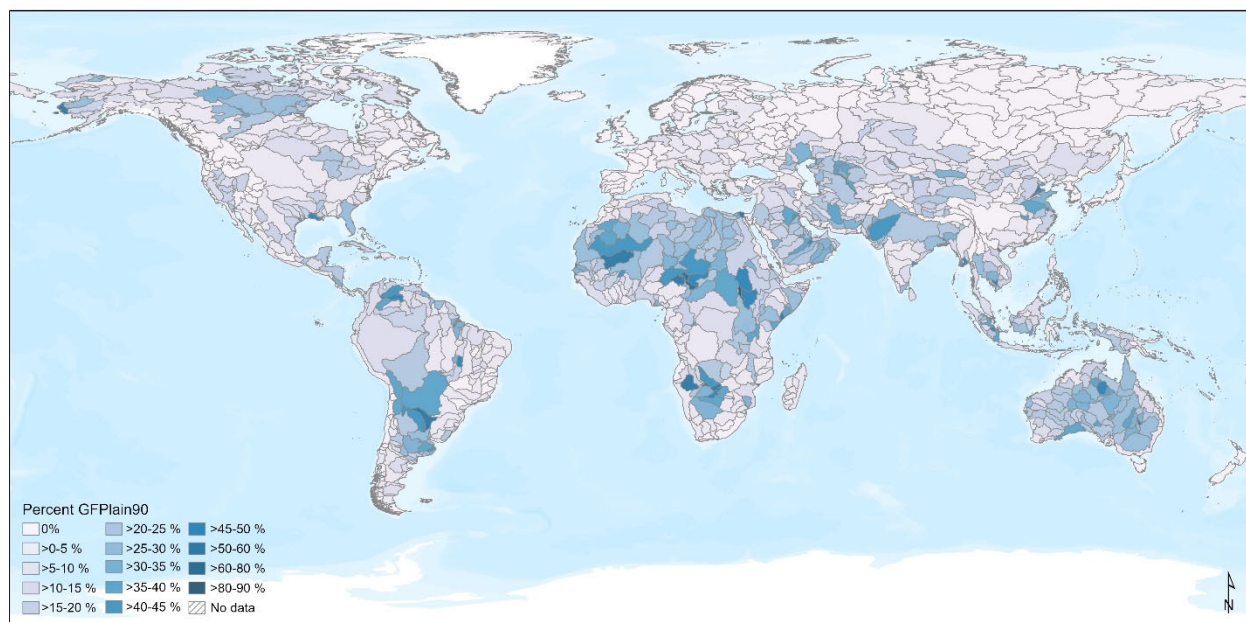
518 **3.3.1 Floodplains**

519

520 Floodplains were estimated to cover 26.6 million km² (Table 5), or 19.7 % of the global landmass.

521 Approximately 23-24 % of the African and Australasian land masses were categorized as occurring

522 within a floodplain, the greatest percentage of global areas so categorized. Conversely, the Arctic
523 (northern Canada and Alaska) and Greenland (excluding the ice sheet) had the least land mass categorized
524 as floodplain (13-14 %). In comparison, Nardi et al. (2019) calculated a global floodplain extent of
525 13,394,139 km², using a 250-m pixel size, a 1000 km² minimum contributing area, and bounding their
526 study between 60° N and 60° S latitudes. Our analyses using the same latitudinal bounds but with a higher
527 resolution dataset (90 m) and a 20 km² minimum contributing area identified 24,185,775 km², an 81 %
528 areal increase (Fig. B1). The relative percent composition of each HydroBASIN that is comprised of
529 GFPlain90 floodplains is given in Fig. 5.
530



531
532 **Figure 5.** Floodplain extents derived from GFPlain90 as a proportion of each of the Level 4 HydroBASINS
533 (Lehrner and Grill, 2013). The data range demonstrated that up to ~90 % of a given watershed was comprised of
534 floodplain area, as evidenced by HydroBASINS in south central Africa and central South America. The basemap
535 layer is the ESRI World Terrain Base (2022).

536
537

538 **Table 5.** Calculated floodplain area for each HydroBASINS at the global scale. Our analyses found 19.7 % of the
 539 landmass occurs within a floodplain.

HydroBASINS Region	Floodplain (km²)	Floodplain Percent of Landmass
Africa	6,990,859	23.3 %
Arctic (northern Canada & Alaska)	894,594	14.2 %
Asia	4,283,991	20.6 %
Australasia	2,649,395	23.8 %
Europe and Middle East	3,415,308	19.1 %
Greenland (excl. ice sheet)	270,813	12.6 %
North & Central America (excl. Alaska)	2,713,346	17.0 %
Siberian Russia	2,051,305	15.8 %
South America	3,368,778	18.9 %
Total	26,638,389	19.7 %

540

541 3.3.2 Wetlands

542

543 Global Wetland extent covered 30.5 million km² (Table 6). With a focus on smaller systems compared to
 544 those presented by Tootchi et al. (2019), our Global Wetland dataset identified 11% more potential global
 545 wetlands (3 million km² additional wetlands). Australasia had the greatest proportional wetland
 546 abundance (see also Zhu et al., 2022), with wetlands covering 38 % of the landmass (driven, in part, by
 547 island abundance and fringing estuarine wetlands [Fan et al., 2013]). Greenland (3 %) and Africa (12 %)
 548 had the least wetlands identified on the land mass.

549

550 **Table 6.** Estimated Global Wetlands areal extent for each of the nine regional HydroBASINS (Lehner and Grill,
 551 2013). As described in the text, Global Wetlands extent incorporates the CW-WTD (Tootchi et al., 2019), CCI
 552 (Herold et al., 2015), and GSW (Pekel et al., 2016); lakes of ≥ 10 ha have been removed (Messenger et al., 2016).

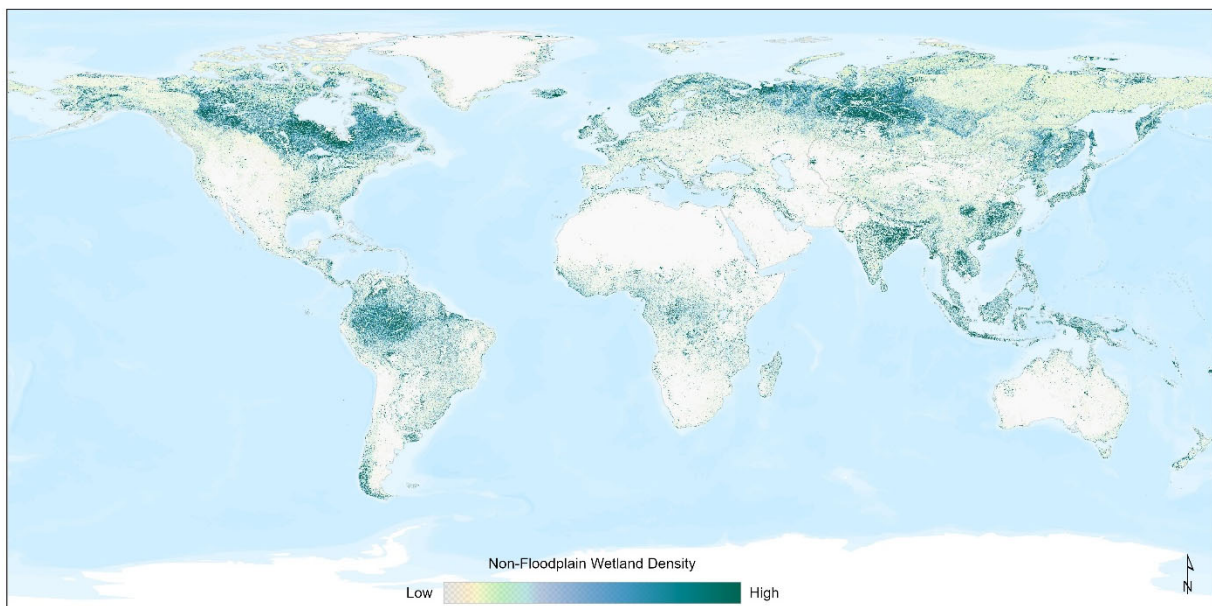
HydroBASINS Region	Wetlands (km²)	Wetland Percent of Landmass
Africa	3,524,917	11.8 %
Arctic (northern Canada & Alaska)	1,807,830	28.6 %
Asia	5,543,333	26.6 %
Australasia	4,283,996	38.4 %
Europe and Middle East	2,465,074	13.8 %
Greenland (excl. ice sheet)	60,761	2.8 %
North & Central America (excl. Alaska)	4,107,333	25.8 %
Siberian Russia	3,578,868	27.6 %
South America	5,140,139	28.8 %
Total	30,512,251	22.6 %

553 3.3.3 Non-floodplain wetlands (Global NFW)

554

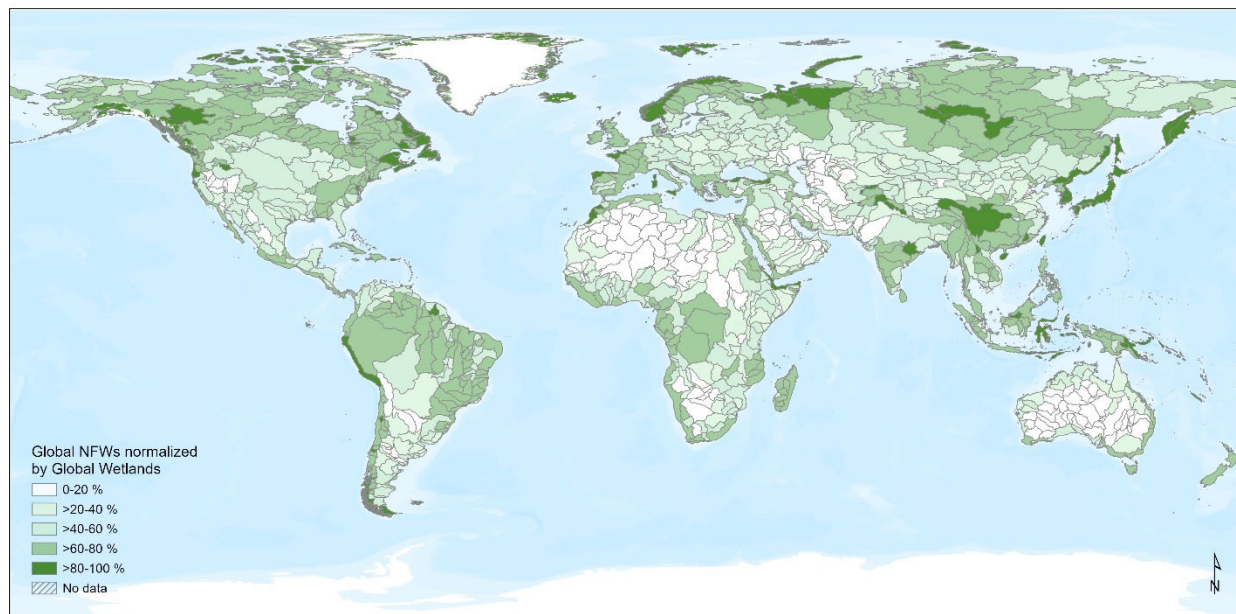
555 Approximately 16.0 million km² of potential non-floodplain wetlands were identified globally (Global
556 NFWs, Fig. 6), meaning that 11.9 % of the global landmass is estimated to be covered by non-floodplain
557 wetlands (Table 7). This represents ~53 % of the total global wetlands found in the dataset used in this
558 analysis (see Methods: Wetland Data, above). The global distribution of non-floodplain wetlands is
559 widespread, though they were found to comprise a higher proportion of wetlands within more northern
560 HydroBASINS watersheds (i.e., higher abundances in formerly glaciated basins), as demonstrated in Fig.
561 7. The Arctic portion of northern Canada and Alaska (21.7 %), and Siberian Russia (17.4 %), typically
562 underlain by permafrost and frequently inundated or saturated due to poor drainage evolution
563 (Kremenetski et al., 2003; Robarts et al., 2013; Olefeldt et al., 2021), had the greatest percent non-

564



565

566 **Figure 6.** Non-floodplain wetlands, Global NFWs, are found worldwide, with a greater abundance in formerly
567 glaciated landscapes of northern climates (e.g., northern North America and Siberian Russia) as well as within the
568 Amazon basin (South America). This density map was created using the Focal Statistics tool in ArcGIS Pro 2.9.1.
569 The basemap layer is the ESRI World Terrain Base (2022).



571

572 **Figure 7.** The proportion of non-floodplain wetlands, Global NFWs, within a given HydroBASINS watershed

573 (Lehrner and Grill, 2013), ranging up to 100 %, varied globally. The impacts or effects of non-floodplain wetlands

574 on biological, biogeochemical, and hydrological functions will vary based on their relative abundance, location

575 within the watershed, and hydrologic characteristics (Lane et al., 2018). The basemap layer is the ESRI World

576 Terrain Base (2022).

577

578 floodplain wetlands. Africa (5.4 %) and Greenland (1.0 %, excluding ice sheets) had the least abundance

579 of non-floodplain wetlands. A four-direction region-group (contagion) analysis conducted to identify

580 adjacent pixels considered as contiguous units or non-floodplain wetland systems identified 32.8 million

581 individual non-floodplain wetlands. Non-floodplain wetlands are typically small aquatic systems (see

582 Table 7): the median size differed across the HydroBASINS regions from 0.018 km² (1.8 ha) to 0.138

583 km² (13.8 ha) with a global median of 0.039 km² (3.87 ha).

584 **Table 7.** Global NFW data further described by HydroBASINS region.

HydroBASINS Region	Global NFW Extent (km²)	Count of Global NFWs (#)	Global NFW Percent of Landmass	Global NFW Median Area (km²)
Africa	1,611,225	2,698,465	5.4 %	0.138
Arctic (northern Canada & Alaska)	1,371,937	5,956,081	21.7 %	0.018
Asia	2,924,900	4,564,172	14.0 %	0.049
Australasia	850,402	1,448,315	7.6 %	0.054
Europe and Middle East	1,475,355	3,740,961	8.3 %	0.054
Greenland (excl. ice sheet)	21,747	180,726	1.0 %	0.018
North & Central America (excl. Alaska)	2,608,158	5,740,066	16.4 %	0.025
Siberian Russia	2,255,689	4,864,577	17.4 %	0.063
South America	2,891,604	3,572,294	16.2 %	0.096
Total	16,011,018	32,765,657	11.9 %	0.039

585

586 **4 Discussion**

587

588 We report here for the first time the global abundance of non-floodplain wetlands, a functionally
 589 important and imperiled resource (Creed et al., 2017). Our estimate of 16.0 million km² suggests that
 590 approximately 53 % of the Earth’s wetlands are likely non-floodplain wetland systems. These aquatic
 591 systems are small, with a range from 0.018-0.138 km² (1.8-13.8 ha) across the globe and a global median
 592 size of 0.039 km² (3.87 ha, see Table 7).

593

594 The global abundance of non-floodplain wetlands is a reasonable first approximation of the total non-
 595 floodplain wetland extent. For instance, non-floodplain wetland estimates in the CONUS were conducted
 596 by Lane et al. (2022) using high-resolution aerial-sourced spatial data layers developed by the National
 597 Wetlands Inventory (U.S. Fish and Wildlife Service, various dates). Lane et al. (2022) reported
 598 approximately 23% of the area of freshwater wetlands to be non-floodplain wetland systems. Yet the
 599 CONUS has lost nearly half of its wetlands since the European colonization (Dahl, 1990), with smaller
 600 and shallower non-floodplain wetlands likely being disproportionately lost (Van Meter and Basu, 2015;
 601 Serran et al., 2017).

602

603 Tootchi et al. (2019) – our base input geospatial data layer – calculated that the global wetland extent
604 identified from incorporating both regularly flooded wetland systems (surface-water and precipitation-
605 sourced) and groundwater-driven wetland systems (e.g., Fan et al., 2013; Hu et al., 2017b) resulted in
606 approximately 27.5 million km² of wetlands, a value towards the higher-end of previously published
607 geospatial wetland datasets (Hu et al., 2017a). In their synthesis, Tootchi et al. (2019) explained their
608 values as particularly influenced by groundwater-driven wetlands, especially those in the tropics (10° N-
609 10° S latitudes, Zhu et al., 2022), following recent studies acknowledging the under-estimation of those
610 wetland systems (e.g. Wania et al., 2013; Gumbrecht et al., 2017).

611
612 It follows that incorporating additional higher-resolution satellite inundation data (Pekel et al., 2016) as
613 well as groundwater-driven wetland systems data (e.g., Fan et al., 2013; Tootchi et al., 2019), as
614 conducted in this study, would similarly maintain the trend towards the higher end in global estimates as
615 found by Hu et al. (2017a) and Tootchi et al. (2019). This is meted out in the simple contrast between the
616 proportional abundance of non-floodplain wetland systems identified here against the 30 m NLCD data
617 product described above (Dewitz, 2019) across the 21 CONUS watersheds in this study. The calculated
618 median watershed abundance of non-floodplain wetlands in both the Global NFWs (9.4 %) and the
619 Tootchi et al. (2019) CW-WTD (9.1 %) datasets from our validation watersheds are nearly 5-fold the
620 abundance of the benchmark data from the NLCD (Table 8). However, this is contrasted with a 7-fold
621 *under-representation* of non-floodplain wetlands as derived from the satellite based GSW data (Table 8,
622 Pekel et al., 2016). This suggests that our first approximation of global non-floodplain wetland estimates
623 may be high, primarily due to the resolution of the input data layers. However, as we discuss below,
624 additional factors than just resolution are likely at play.

625
626 It is apparent that the GSW alone is insufficient to map non-floodplain wetlands (this study, Vanderhoof
627 and Lane, 2019). Though useful as a satellite-based input data layer, the GSW by itself appears
628 inadequate for identifying non-floodplain wetlands because it relies on surface-water inundation and

629 ignores saturated wetland systems and those driven by groundwater discharge and upwelling (Winter et
630 al., 1998). Fan et al. (2013) found that groundwater drivers of aquatic system state were important and
631 underrepresented in global datasets. Relying on surface water inundation captured during satellite
632 overflights depends not only on an unobstructed view of the waterbody (e.g., not obscured by trees) but
633 also fortuitous timing regarding inundation status. For example, in an analysis of non-floodplain wetlands
634 of the CONUS as derived by distance from an aquatic system, Lane and D'Amico (2016) reported that
635 just over 50 % of the non-floodplain wetlands were classified as seasonally or temporarily flooded –
636 meaning that cloud-free and unobscured overflights would only potentially identify these systems at
637

638 **Table 8.** A comparison of the non-floodplain wetland distribution within the 21 HUCs contrasting across NLCD
639 (the benchmark data layer, Dewitz, 2019), Global NFW (this study), CW-WTD (Tootchi et al., 2019), and GSW
640 (Pekel et al., 2016). The CW-WTD (at 500 m) and the Global NFW (coupling 500 m, 300 m, and 30 m data),
641 derived from the CW-WTD, identified 5-fold the abundance of non-floodplain wetlands whereas the GSW under-
642 estimated non-floodplain wetlands nearly 7-fold.

HUC ID	Percent HUC as			
	NLCD NFW	Global NFW	CW-WTD NFW	GSW NFW
HUC_0101	10.4 %	19.2 %	18.9 %	0.1 %
HUC_0103	8.1 %	14.6 %	14.3 %	0.2 %
HUC_0106	8.2 %	8.0 %	7.5 %	0.3 %
HUC_0203	4.9 %	8.4 %	8.3 %	0.4 %
HUC_0208	4.7 %	12.0 %	11.5 %	4.6 %
HUC_0304	12.2 %	21.7 %	20.8 %	12.2 %
HUC_0313	8.3 %	14.4 %	13.5 %	8.2 %
HUC_0501	1.5 %	9.2 %	8.9 %	0.1 %
HUC_0706	0.7 %	9.7 %	9.5 %	0.3 %
HUC_0804	9.7 %	17.1 %	16.2 %	9.7 %
HUC_1003	0.7 %	2.1 %	1.9 %	0.2 %
HUC_1015	1.8 %	2.0 %	1.3 %	0.1 %
HUC_1016	3.6 %	16.6 %	15.5 %	2.6 %
HUC_1024	0.5 %	5.1 %	4.9 %	0.2 %
HUC_1029	0.9 %	8.4 %	7.7 %	0.4 %
HUC_1304	0.0 %	5.5 %	5.5 %	0.0 %
HUC_1601	0.7 %	1.3 %	1.0 %	0.1 %
HUC_1708	2.0 %	11.7 %	11.6 %	0.4 %
HUC_1711	1.8 %	9.4 %	9.1 %	0.2 %
HUC_1805	2.2 %	9.9 %	9.7 %	0.5 %
HUC_1808	0.3 %	1.7 %	1.6 %	0.1 %
Median	2.0 %	9.4 %	9.1 %	0.3 %

643

644 certain inundated times of the year. Additionally, Lane and D'Amico (2016) identified another 6 % of
645 CONUS non-floodplain wetlands as saturated (i.e., wetlands with saturated substrates but with surface
646 water seldom present). These wetlands would not be identified by the GSW (Pekel et al., 2016) resulting
647 in a further under-representation of the global resource. Similarly, Hamunyela et al. (2022), analyzing
648 ~150,000 km² in southeastern Africa, found that the GSW underestimated surface water extent (i.e.,
649 omission errors) by nearly 65%. Vanderhoof and Lane (2019) found approximately 42% omission rates
650 when contrasting the GSW data to surface-water extent in non-floodplain wetlands ranging from 0.2-17.6
651 ha in area in the Midwestern US. While the GSW is an outstanding dataset that is continuing to be
652 managed and updated, the GSW and its derived product have limitations in their stand-alone utility in
653 global non-floodplain wetland analyses.

654
655 While solely using satellite-based surface-water data products omits groundwater-driven and saturated
656 wetlands and likely results in non-floodplain wetland underestimations, our Global Wetland data
657 incorporated the finer-resolution CCI (Herold et al., 2015) and GSW (Pekel et al., 2016) products into the
658 Tootchi et al. (2019) base map, substantially improving wetland identification (see Table 3). These
659 improvements, as indicated by performance indices increasing from 10-50 % in the derived Global NFW
660 data (see Table 4), support the inclusion of these higher-resolution satellite-based data (Herold et al.,
661 2015; Pekel et al., 2016) with groundwater datasets (Fan et al., 2013), especially when focused on smaller
662 and non-floodplain wetland systems. Similarly, at a coarser scale of 1 km, there was a difference in Mean
663 Absolute Error value of 0.09 (see Table 4) between the Global NFWs and the benchmark NLCD. This ~9
664 % difference between the two datasets at a 1 km resolution (the former originating at 500 m and the latter
665 at 30 m) further suggest substantive potential utility in these global non-floodplain wetland data for
666 effective natural resource management and decision-making.

667

668

669 **5 Implications**

670

671 Non-floodplain wetlands remain vulnerable waters (Creed et al., 2017), despite the fact that the
672 hydrological, biogeochemical, and biological functions performed by non-floodplain wetlands are
673 increasingly noted in the literature (e.g., Leibowitz, 2003; Creed et al., 2017; Lane et al., 2018; Lane et
674 al., 2022), incorporated into eco-hydrological models by the scientific community (e.g., Fossey and
675 Rousseau, 2016; Golden et al., 2017; Golden et al., 2021; Leibowitz et al., 2023), and considered by
676 policy makers (e.g., Biggs et al., 2017; Drenkhan et al., 2022). Their global fate has important
677 implications for watershed-scale resilience to changing climatic conditions (Mckenna et al., 2017; Lane et
678 al., 2022) affecting the measured benefits humans receive from biogeochemical processing, stormwater
679 attenuation, and drought mitigation functions provided by non-floodplain wetlands.

680

681 Global attention to functions of non-floodplain wetlands has increased in the United States (Marton et al.,
682 2015; Rains et al., 2016; Cohen et al., 2016), Europe (Biggs et al., 2017; Nitzsche et al., 2017; Rodríguez-
683 Rodríguez et al., 2021), Asia (Kam, 2010; Van Meter et al., 2014), Australia (Adame et al., 2019), Africa
684 (Merken et al., 2015; Samways et al., 2020), South America (Rodrigues et al., 2012; Cunha et al., 2019)
685 and elsewhere (see extensive review in Chen et al., 2022). This includes analyses of non-floodplain
686 wetlands both as individual systems (e.g., assessing the functions of a single wetland or wetland complex;
687 Badiou et al., 2018) as well as agglomerated, watershed-scale functioning systems (e.g., answering
688 questions on the functional contributions of all non-floodplain wetlands at larger spatial extents; Golden
689 et al., 2016; Blanchette et al., 2022). Previous studies found that non-floodplain wetlands are
690 overwhelmingly important contributors to biogeochemical and hydrological functions affecting
691 downgradient (i.e., down-stream) water quality and streamflow (e.g., McLaughlin et al., 2014; Marton et
692 al., 2015; Cohen et al., 2016; Rains et al., 2016; Golden et al., 2019; Cheng et al., 2020). Hence, with the
693 development of this publicly available dataset, and subsequent improvements by others, it is hoped that

694 these important aquatic systems will be incorporated into resource management and decision-making
695 across the globe.

696
697 Recently, Lane et al. (2022) identified global-scale geospatial data of the spatial extent and spatial
698 configuration of vulnerable waters – non-floodplain wetlands and headwater stream systems (e.g.,
699 ephemeral, intermittent, and perennial low-order waters [Strahler, 1957]) – as a critical scientific gap.
700 Discounting their significance in watershed-scale hydrology and nutrient biogeochemistry analyses – as
701 well as their importance in biological processes (Schofield et al., 2018; Smith et al., 2019; Mushet et al.,
702 2019) – affects quantification of the myriad ecosystem services they provide (De Groot, 2006; Colvin et
703 al., 2019). For instance, Golden et al. (2021) provide a tangible example of the functional effects and
704 influence of non-floodplain wetlands once incorporated into watershed-scale hydrologic models (Fig. 8):
705 ignoring non-floodplain wetlands in the model resulted in projected critical flood-stage return intervals
706 (e.g., 50 yr and 100 yr floods) being reached within a given modeled time frame. Conversely,
707 incorporating non-floodplain wetlands and their storage capacities into a river basin model (e.g., Rajib et
708 al., 2020) demonstrated that non-floodplain wetlands significantly attenuate storm flows, for when non-
709 floodplain wetlands are “...integrated into the model, those simulated *flood stages are not reached*”
710 (Golden et al., 2021, p. 3, emphasis added). The hydrological functions and concomitantly the associated
711 biogeochemical functions (e.g., Marton et al., 2015) of non-floodplain wetlands demand an effective
712 accounting of their spatial extent and configuration, as demonstrated in this novel global dataset.

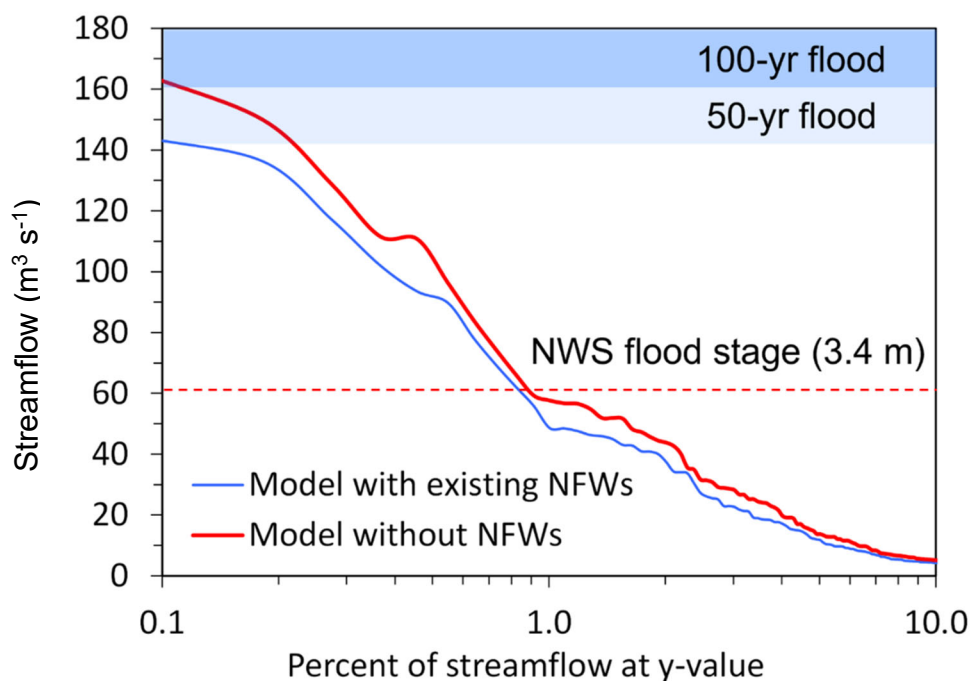
713

714 **6 Global Non-Floodplain Wetlands: Continuing advancements and conclusion**

715

716 Noting the challenges in accurately identifying non-floodplain wetlands – including small size, frequent
717 non-perennial hydrological inundation, soil saturation rather than overlying surface water, and canopy or
718 cloud cover obstructing satellite or airborne detection – recommendations for advanced analyses of non-
719 floodplain wetland extent hinge initially on the use of ancillary data sources. For instance, global

720 assessments will be improved through wall-to-wall high resolution digital elevation models that are used
 721 to identify depressions on the landscape (e.g., Wu et al., 2019b). Though not all landscape depressions are
 722 non-floodplain wetlands (or wetlands at all), analyses that include depressions may find improved
 723 performance when used in combination with vegetation-based assessments or spectral analyses
 724 identifying water (Devries et al., 2017; Evenson et al., 2018b). Similarly, emerging synthetic aperture
 725 radar-based landscape classifications (e.g., Huang et al., 2018; Martinis et al., 2022; Brown et al., 2022)
 726 and both airborne and satellite-borne hyperspectral and advanced analyses, including LiDAR, as well as
 727
 728



729
 730 **Figure 8.** Non-floodplain wetlands attenuate storm flows and decrease flooding hazards. In this example from
 731 Golden et al. (2021, used by permission under Creative Commons Attribution 4.0 license), incorporating the
 732 floodwater storage and attenuation functions of non-floodplain wetlands (NFWs, here) resulted in substantive
 733 decreases in flood-stage heights (i.e., modeled stream outcomes incorporating non-floodplain wetlands reached
 734 neither 50 yr nor 100 yr floods extents). The data from Golden et al. (2021) is of USGS Pipestem Creek gage
 735 06469400, draining approximately 1,800 km².

736 analytical capabilities (e.g., machine-learning approaches, object-oriented classifications, Berhane et al.,
737 2018); topographically based models, Xi et al., 2022; see Table B1) hold great promise for improved
738 resolution and performance in identifying non-floodplain wetlands (Christensen et al., 2022).

739
740 The Global NFW dataset is not perfect, yet it incrementally advances the current understanding of the
741 potential extent of this important aquatic resource. Limitations of the global dataset (see also Section 4)
742 include the error-propagation and imperfections of the input data layers, including the relatively coarse
743 nature of four of the main input data layers (i.e., the 1000 m groundwater data from Fan et al. (2013), 500
744 m CW-WTD from Tootchi et al. (2019), 500 m GIEMS-D15 from Fluet-Chouinard et al. (2015), and the
745 300 m CCI from Herold et al. (2015)) relative to the target wetland size as clearly evident in Fig. 4. We
746 additionally acknowledge that omission and commission errors remain within this global data product.
747 For instance, our floodplain-masking process may have inadvertently misassigned pixels derived at 500 m
748 into either non-floodplain or floodplain groups. Though data were not lost when we resampled
749 downwards to 30 m from 500 m, the topological relationships were not necessarily maintained, adding
750 error to the determination of floodplain or non-floodplain pixel status (especially as it relates to those
751 pixels proximate to floodplains). Though imperfect, we suggest Global NFW data should be cautiously
752 incorporated into hydrological, biogeochemical, and biological models to account for the important
753 functions non-floodplain wetlands perform.

754
755 Similarly, though this Global NFW is a static data layer, land use, development, and climate changes
756 continue to affect the prevalence of wetlands worldwide. Fluet-Chouinard et al. (2023) recently noted a
757 global wetland loss of 21% since 1700, with rapid increases from 1950s onwards. Returning to the
758 identification of wetlands and their spatial location vis-à-vis floodplains, using the preponderance of
759 higher-resolution (i.e., < 30 m) and high-return interval sensors will improve both the spatial and
760 temporal accuracy of these data, decreasing commission and omission errors (e.g., Table 8) while

761 increasing the accurate identification of smaller aquatic features that occasional cease to hold standing
762 water.

763
764 The keys to quantifying the functional contributions, ecosystem services, and watershed-scale resilience
765 conferred by non-floodplain wetlands through hydrological, biogeochemical, and biological processes are
766 found through, as a first principle, identifying the spatial extent and configuration of this disappearing and
767 imperiled aquatic system (Creed et al., 2017; Lane et al., 2022). This novel geospatial dataset, freely
768 available (https://gaftp.epa.gov/EPADDataCommons/ORD/Global_NonFloodplain_Wetlands/, Lane et al.,
769 2023), provides for sustainable management of an important aquatic resource and advances the global
770 assessment of non-floodplain wetland functions by facilitating non-floodplain wetland inclusion in both
771 existing models and those under development (Golden et al., 2021).

772

773 **7 Data availability**

774

775 The data are available on the United State Environmental Protection Agency’s Environmental Dataset
776 Gateway (DOI: <https://doi.org/10.23719/1528331>, Lane et al., 2023) or
777 https://gaftp.epa.gov/EPADDataCommons/ORD/Global_NonFloodplain_Wetlands/, (last accessed
778 12/06/2022). Here, we provide global gridded floodplain (90 m, GFPLain90, ~/Global_Floodplains),
779 global gridded wetlands (30 m, Global Wetlands, ~/Global_Wetlands), and global gridded non-floodplain
780 wetlands (30 m, Global NFWs, ~/Global_NFWs) for each of the 3142 HydroBASINS, organized by
781 HydroBASINS region (see, e.g., Table 7).

782

783 **Author contributions.** CL, JC, HG, and ED conceptualized the study, developed the formal analysis, and
784 conducted and/or assisted the data validation. CL wrote and edited the manuscript, while JC and HG
785 reviewed and edited the manuscript. ED also developed the methodology, curated the data, conducted the
786 formal spatial analysis, validated the data, visualized the data, and reviewed and edited the manuscript.

787 QW and AR assisted in methodology development, validated the study outputs, conducted formal
788 analyses, and reviewed and edited the manuscript.

789
790 **Competing interests.** The corresponding authors have declared that none of the authors have any
791 competing interests.

792
793 **Disclaimer.** Publisher’s note: Copernicus Publications remains neutral with regard to jurisdictional
794 claims in published maps and institutional affiliations.

795
796 **Acknowledgements.** We greatly appreciate the scientific contributions and stimulative discussions in the
797 papers led by Ardalan Tootchi, Sean Woznicki, Fernando Nardi, Oliver Wing, Paul Bates, and their co-
798 authors that inspired us to complete these analyses. Jeremy Baynes and John Johnston conducted critical
799 reviews to improve this manuscript, and their efforts are acknowledged. This paper has been reviewed in
800 accordance with the US Environmental Protection Agency’s peer and administrative review policies and
801 approved for publication. Mention of trade names or commercial products does not constitute
802 endorsement or recommendation for use. Statements in this publication reflect the authors’ professional
803 views and opinions and should not be construed to represent any determination or policy of the US
804 Environmental Protection Agency.

805
806 **Review statement.** This paper was edited by Yuanzhi Yao and reviewed by Youjiang Shen and Michele
807 Ronco.

808
809 **Appendix A: Abbreviations**

810	AEB	Aggregate error bias
811	CaMa-Flood	Catchment-based Macro-scale Floodplain
812	CCI	Climate change initiative

813	CIMA-UNEP	CIMA Research Foundation - United Nations Environmental Programme
814	CONUS	Conterminous United States
815	CSI	Critical Success Index
816	CW-WTD	Composite wetland-water table depth
817	DEM	Digital elevation model
818	EB	Error Bias
819	ECMWF	European Centre for Medium-Range Weather Forecasts
820	EPA	Environmental Protection Agency
821	ESA	European Space Agency
822	FA	False Alarm
823	FEMA	Federal Emergency Management Agency
824	GDW	Groundwater-driven wetlands
825	GFPlain	Global Floodplain
826	GIEMS-D15	Global Inundation Extent from Multi-Satellites Downscaled - 15 arcseconds
827	GIS	Geographic information systems
828	GLOFRIS	Global Flood Risk with Image Scenarios
829	GLWD	Global Lakes and Wetlands Database
830	GNFW	Global Non-floodplain wetlands
831	GSW	Global surface water
832	GW	Global wetlands
833	H	Hit Rate
834	HUC	Hydrologic unit code
835	IPCC	Intergovernmental Panel on Climate Change
836	JRC	Joint Research Center
837	LIDAR	Light detection and ranging
838	MAE	Mean absolute error

839	MERIT	Multi-Error Removed Improved Terrain
840	ML	Machine learning
841	NFW	Non-floodplain wetland
842	NLCD	National Land Cover Database
843	NWS	National Weather Service
844	P	Precision
845	RFW	Regularly flooded wetland
846	SAR	Synthetic aperture radar
847	USA	United States of America
848	USGS	United States Geological Survey
849	UTM	Universal Transverse Mercator
850	WTD	Water table depth
851		

852 **Appendix B: Supplemental Tables and Figures**

853 **Table B1.** Emerging global land cover datasets related to surface water and wetlands.

Data Set	Resolution	Years of Data	Wetland Classes	Image Sources	Reference and website
ESA WorldCover	10 m	2020-2021	Permanent water bodies; herbaceous wetland; mangroves	Sentinel-1 & Sentinel-2	Zanaga et al. (2021); https://esa-worldcover.org
Esri Global Land Cover	10 m	2017-2022	Water; flooded vegetation	Sentinel-2	Karra et al. (2021); https://livingatlas.arcgis.com/landcover
Dynamic World	10 m	2015-2023	Water; flooded vegetation	Sentinel-2	Brown et al. (2022); https://dynamicworld.app/

854

855

856 **Table B2.** Descriptive characteristics of the 21 verification basins located throughout the CONUS (see Fig. 2).
857 Majority Köppen-Geiger classification follows Beck et al. (2018). Climatological data were acquired from the
858 PRISM Climate Group (Parameter-elevation Regressions on Independent Slopes Model, prism.oregonstate.edu/,
859 accessed 09/26/2022) using the 30-year annual normals for each watershed. Land use data and descriptions are from
860 the 2019 NLCD (www.mrlc.gov/data, accessed 09/26/2022) and represent the land use class with the greatest areal
861 abundance. Average elevation was derived from the USGS National Elevation Dataset (https://www.usgs.gov/3d-
862 elevation-program, accessed 01/13/2022). Global Wetland Count are the counts of wetlands from the derived Global
863 Wetland database within each watershed after region-grouping the data using a four-direction contagion criterion
864 (i.e., pixels immediately adjacent in any of the four cardinal directions are considered part of a unique, multi-pixel
865 wetland, ArcGIS Pro v.2.9.1, Redlands, California).

Hydrologic Unit Code	Area	Köppen-	Mean Annual	Mean Annual
ID	(km ²)	Geiger	Temp (°C)	Rainfall (m)
HUC_0101	18,906	Dfb	4.0	1.1
HUC_0103	15,287	Dfb	5.4	1.2
HUC_0106	10,800	Dfb	7.5	1.3
HUC_0203	12,490	Dfa	11.6	1.2
HUC_0208	47,449	Cfa	13.7	1.2
HUC_0304	47,899	Cfa	16.4	1.3
HUC_0313	52,169	Cfa	18.1	1.4
HUC_0501	30,371	Dfb	8.6	1.2
HUC_0706	22,257	Dfa	8.1	1.0
HUC_0804	53,108	Cfa	17.5	1.4
HUC_1003	51,431	BSk	5.6	0.4
HUC_1015	37,098	Dfa	8.7	0.5
HUC_1016	54,743	Dfa	6.4	0.6
HUC_1024	35,237	Dfa	10.8	0.9
HUC_1029	48,204	Dfa	13.2	1.1
HUC_1304	48,126	BSh	18.6	0.4
HUC_1601	19,463	BSk	5.7	0.5
HUC_1708	16,101	Csb	9.0	2.1
HUC_1711	35,651	Csb	8.2	2.0
HUC_1805	11,341	Csb	14.9	0.7
HUC_1808	11,789	BSk	8.4	0.4

866 † Köppen-Geiger Class Descriptions (Beck et al. 2018): BSh (arid, steppe, hot), BSk (arid, steppe, cold), Cfa
867 (temperate, no dry season, hot summer), Csb, (temperature, dry season, warm summer), Dfa (cold, no dry season,
868 hot summer), Dfb (cold, no dry season, warm summer)

869

870 **Table B2.** (Continued)

Hydrologic Unit	Majority Land	Majority Land	Global Wetland	Average
Code	Use Coverage	Coverage Description	Count	Elevation
HUC_0101	43	Mixed Forest	2,141	296
HUC_0103	43	Mixed Forest	2,202	300
HUC_0106	43	Mixed Forest	2,799	169
HUC_0203	41	Deciduous Forest	2,438	82
HUC_0208	41	Deciduous Forest	13,934	187
HUC_0304	90	Woody Wetlands	14,643	127
HUC_0313	42	Evergreen Forest	27,056	147
HUC_0501	41	Deciduous Forest	6,310	484
HUC_0706	82	Cultivated Crops	3,100	300
HUC_0804	42	Evergreen Forest	12,242	85
HUC_1003	71	Herbaceous	11,852	1349
HUC_1015	71	Herbaceous	8,628	961
HUC_1016	82	Cultivated Crops	61,482	464
HUC_1024	82	Cultivated Crops	11,995	341
HUC_1029	81	Hay/Pasture	23,935	297
HUC_1304	52	Shrub/Scrub	1,733	995
HUC_1601	52	Shrub/Scrub	2,642	1981
HUC_1708	42	Evergreen Forest	1,986	552
HUC_1711	42	Evergreen Forest	6,562	621
HUC_1805	52	Shrub/Scrub	1,208	222
HUC_1808	52	Shrub/Scrub	1,089	1625

871

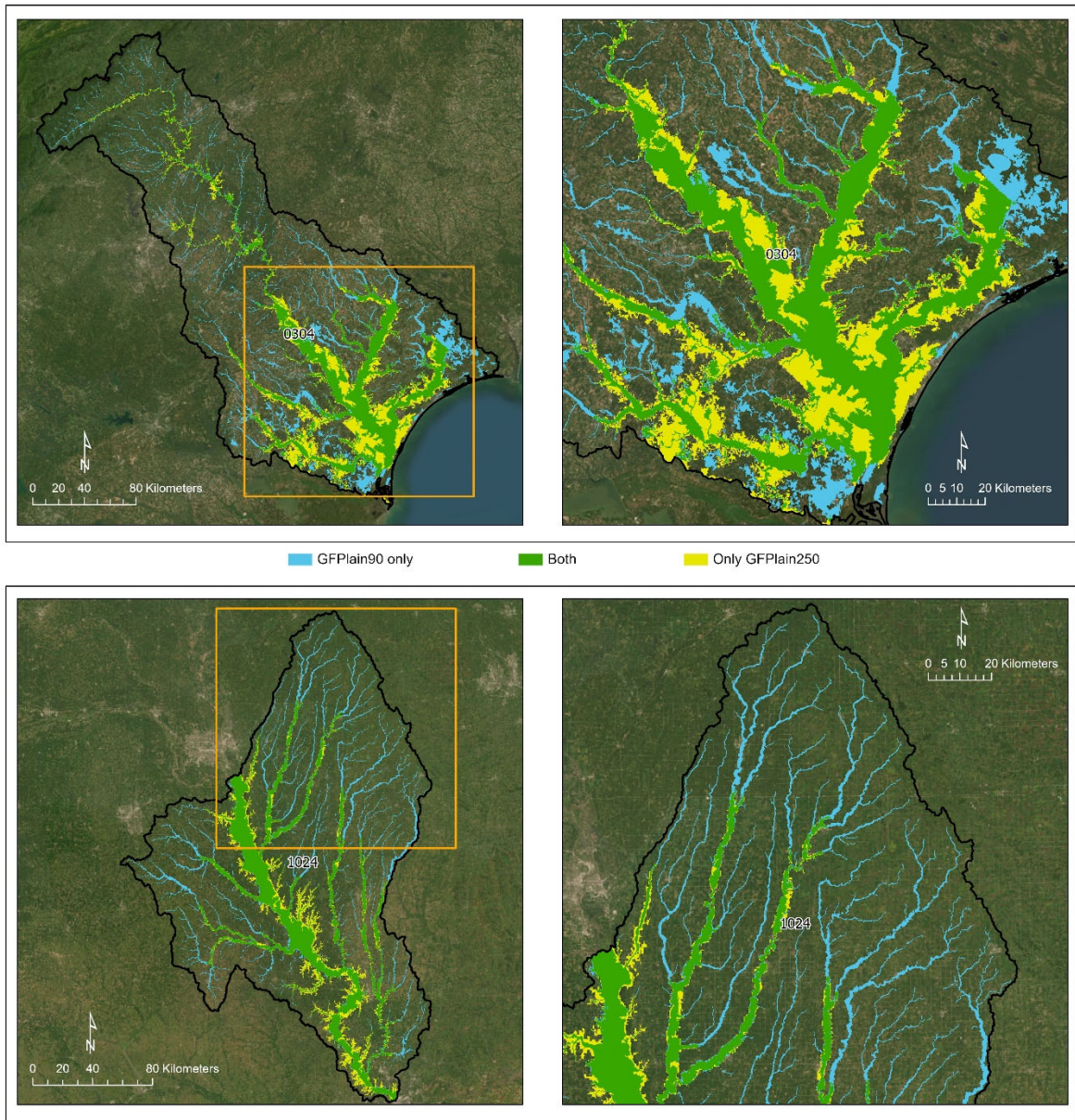
872

873 **Table B3.** Floodplain performance assessment of the GFPlain90-derived floodplain and the benchmark floodplain
874 from Woznicki et al. (2019). The first six equations directly assess the spatial concordance and overlap between the
875 two datasets, whereas Mean Absolute Error (Eq. 7) and Aggregate Error Bias (Eq. 8) are coarser fractional analyses
876 (i.e., the fraction of a 1 km² cell predicted correctly) as measured along the riverine network.

Hydrologic Unit Code (HUC) ID	Hit Rate	Precision	False Alarm	CSI	F1	Error Bias	Mean Absolute Error	Aggregate Error Bias
	(Eq. 1)	(Eq. 2)	(Eq. 3)	(Eq. 4)	(Eq. 5)	(Eq. 6)	(Eq. 7)	(Eq. 8)
HUC_0101	0.76	0.84	0.16	0.66	0.80	0.62	0.06	-0.01
HUC_0103	0.92	0.77	0.23	0.72	0.84	3.25	0.05	0.03
HUC_0106	0.78	0.74	0.26	0.62	0.76	1.24	0.10	-0.03
HUC_0203	0.47	0.58	0.42	0.35	0.52	0.66	0.25	-0.18
HUC_0208	0.64	0.73	0.27	0.52	0.68	0.67	0.13	-0.08
HUC_0304	0.63	0.81	0.19	0.55	0.71	0.41	0.06	0.00
HUC_0313	0.62	0.72	0.28	0.50	0.67	0.62	0.09	-0.01
HUC_0501	0.77	0.85	0.15	0.68	0.81	0.59	0.04	-0.02
HUC_0706	0.86	0.79	0.21	0.69	0.82	1.62	0.04	0.02
HUC_0804	0.75	0.83	0.17	0.65	0.79	0.64	0.08	-0.02
HUC_1003	0.85	0.42	0.58	0.39	0.56	7.70	0.11	0.09
HUC_1015	0.81	0.74	0.26	0.63	0.78	1.54	0.06	0.02
HUC_1016	0.89	0.36	0.64	0.35	0.52	14.79	0.18	0.17
HUC_1024	0.90	0.88	0.12	0.80	0.89	1.19	0.03	0.00
HUC_1029	0.84	0.87	0.13	0.75	0.85	0.82	0.04	-0.01
HUC_1304	0.66	0.74	0.26	0.53	0.70	0.67	0.07	-0.01
HUC_1601	0.92	0.55	0.45	0.52	0.69	9.47	0.10	0.08
HUC_1708	0.60	0.71	0.29	0.48	0.65	0.60	0.08	-0.03
HUC_1711	0.70	0.50	0.50	0.41	0.58	2.25	0.10	-0.02
HUC_1805	0.59	0.59	0.41	0.41	0.59	1.00	0.14	-0.05
HUC_1808	0.98	0.44	0.56	0.44	0.61	82.97	0.24	0.23
Median	0.77	0.74	0.26	0.53	0.70	1.00	0.08	-0.01
Mean	0.76	0.69	0.31	0.56	0.71	6.35	0.10	0.01

877

878



879

880 **Figure B1.** Comparison of floodplain extents derived from GFPlain90 (this study) and GFPlain250 (Nardi et al.,
 881 2019). The right-hand panels are the inset area outlined in the orange box on the left panels; the top panels represent
 882 an eastern coastal watershed (HUC_0304) whereas the bottom panels are from a midwestern US watershed
 883 (HUC_1024). The full extent of the riverine network is evident in the GFPlain90 dataset, which was derived from 90
 884 m resolution DEMs in contrast to the 250 m pixel size of the GFPlain250. Satellite imagery sourced from ESRI
 885 (2022).

886 **References**

887

888 Adame, M. F., Arthington, A. H., Waltham, N., Hasan, S., Selles, A., and Ronan, M.: Managing threats
889 and restoring wetlands within catchments of the Great Barrier Reef, Australia, *Aquatic Conservation:
890 Marine and Freshwater Ecosystems*, 29, 829-839, <https://doi.org/10.1002/aqc.3096>, 2019.

891 Alfieri, L., Salamon, P., Bianchi, A., Neal, J., Bates, P., and Feyen, L.: Advances in pan-European flood
892 hazard mapping, *Hydrological Processes*, 28, 4067-4077, 10.1002/hyp.9947, 2014.

893 Ameli, A. A. and Creed, I. F.: Does Wetland Location Matter When Managing Wetlands for Watershed-
894 Scale Flood and Drought Resilience?, *JAWRA Journal of the American Water Resources Association*,
895 55, 529-542, 10.1111/1752-1688.12737, 2019.

896 Aronica, G., Bates, P. D., and Horritt, M. S.: Assessing the uncertainty in distributed model predictions
897 using observed binary pattern information within GLUE, *Hydrological Processes*, 16, 2001-2016,
898 <https://doi.org/10.1002/hyp.398>, 2002.

899 Assessment, M. E.: *Ecosystems and Human Well-Being: Wetlands and Water Synthesis*, World
900 Resources Institute, Washington, D.C., 2005.

901 Badiou, P., Page, B., and Akinremi, W.: Phosphorus Retention in Intact and Drained Prairie Wetland
902 Basins: Implications for Nutrient Export, *Journal of Environmental Quality*, 47, 902-913,
903 <https://doi.org/10.2134/jeq2017.08.0336>, 2018.

904 Bam, E. K. P., Ireson, A. M., van der Kamp, G., and Hendry, J. M.: Ephemeral Ponds: Are They the
905 Dominant Source of Depression-Focused Groundwater Recharge?, *Water Resources Research*, 56,
906 e2019WR026640, <https://doi.org/10.1029/2019WR026640>, 2020.

907 Bates, P. D. and De Roo, A. P. J.: A simple raster-based model for flood inundation simulation, *Journal of*
908 *Hydrology*, 236, 54-77, [http://dx.doi.org/10.1016/S0022-1694\(00\)00278-X](http://dx.doi.org/10.1016/S0022-1694(00)00278-X), 2000.

909 Beck, H. E., Zimmermann, N. E., McVicar, T. R., Vergopolan, N., Berg, A., and Wood, E. F.: Present
910 and future Köppen-Geiger climate classification maps at 1-km resolution, *Scientific Data*, 5, 180214,
911 10.1038/sdata.2018.214, 2018.

912 Berhane, T., Lane, C., Wu, Q., Autrey, B., Anenkhonov, O., Chepinoga, V., and Liu, H.: Decision-Tree,
913 Rule-Based, and Random Forest Classification of High-Resolution Multispectral Imagery for Wetland
914 Mapping and Inventory, *Remote Sensing*, 10, 580, 2018.

915 Biggs, J., von Fumetti, S., and Kelly-Quinn, M.: The importance of small waterbodies for biodiversity
916 and ecosystem services: implications for policy makers, *Hydrobiologia*, 793, 3-39, 10.1007/s10750-
917 016-3007-0, 2017.

918 Blanchette, M., Rousseau, A. N., Savary, S., and Foulon, É.: Are spatial distribution and aggregation of
919 wetlands reliable indicators of stream flow mitigation?, *Journal of Hydrology*, 608, 127646,
920 <https://doi.org/10.1016/j.jhydrol.2022.127646>, 2022.

921 Brown, C. F., Brumby, S. P., Guzder-Williams, B., Birch, T., Hyde, S. B., Mazzariello, J., Czerwinski,
922 W., Pasquarella, V. J., Haertel, R., Ilyushchenko, S., Schwehr, K., Weisse, M., Stolle, F., Hanson, C.,
923 Guinan, O., Moore, R., and Tait, A. M.: Dynamic World, Near real-time global 10 m land use land
924 cover mapping, *Scientific Data*, 9, 251, 10.1038/s41597-022-01307-4, 2022.

925 Buttle, J. M.: Mediating stream baseflow response to climate change: The role of basin storage,
926 *Hydrological Processes*, 32, 363-378, 10.1002/hyp.11418, 2018.

927 Chen, J., Chen, J., Liao, A., Cao, X., Chen, L., Chen, X., He, C., Han, G., Peng, S., Lu, M., Zhang, W.,
928 Tong, X., and Mills, J.: Global land cover mapping at 30m resolution: A POK-based operational
929 approach, *ISPRS Journal of Photogrammetry and Remote Sensing*, 103, 7-27,
930 <https://doi.org/10.1016/j.isprsjprs.2014.09.002>, 2015.

931 Chen, W., Thorslund, J., Nover, D. M., Rains, M. C., Li, X., Xu, B., He, B., Su, H., Yen, H., Liu, L.,
932 Yuan, H., Jarsjö, J., and Viers, J. H.: A typological framework of non-floodplain wetlands for global
933 collaborative research and sustainable use, *Environmental Research Letters*, 17, 113002, 10.1088/1748-
934 9326/ac9850, 2022.

935 Cheng, F. Y. and Basu, N. B.: Biogeochemical hotspots: Role of small water bodies in landscape nutrient
936 processing, *Water Resources Research*, 53, 5038-5056, 10.1002/2016WR020102, 2017.

937 Cheng, F. Y., Van Meter, K. J., Byrnes, D. K., and Basu, N. B.: Maximizing US nitrate removal through
938 wetland protection and restoration, *Nature*, 588, 625-630, 10.1038/s41586-020-03042-5, 2020.

939 Christensen, J. R., Golden, H. E., Alexander, L. C., Pickard, B. R., Fritz, K. M., Lane, C. R., Weber, M.
940 H., Kwok, R. M., and Keefer, M. N.: Headwater streams and inland wetlands: Status and advancements
941 of geospatial datasets and maps across the United States, *Earth-Science Reviews*, 104230,
942 <https://doi.org/10.1016/j.earscirev.2022.104230>, 2022.

943 Cohen, M. J., Creed, I. F., Alexander, L., Basu, N. B., Calhoun, A. J. K., Craft, C., D'Amico, E.,
944 DeKeyser, E., Fowler, L., Golden, H. E., Jawitz, J. W., Kalla, P., Kirkman, L. K., Lane, C. R., Lang,
945 M., Leibowitz, S. G., Lewis, D. B., Marton, J., McLaughlin, D. L., Mushet, D. M., Raanan-Kiperwas,
946 H., Rains, M. C., Smith, L., and Walls, S. C.: Do geographically isolated wetlands influence landscape
947 functions?, *Proceedings of the National Academy of Sciences*, 113, 1978-1986,
948 10.1073/pnas.1512650113, 2016.

949 Colvin, S. A. R., Sullivan, S. M. P., Shirey, P. D., Colvin, R. W., Winemiller, K. O., Hughes, R. M.,
950 Fausch, K. D., Infante, D. M., Olden, J. D., Bestgen, K. R., Danehy, R. J., and Eby, L.: Headwater
951 Streams and Wetlands are Critical for Sustaining Fish, Fisheries, and Ecosystem Services, *Fisheries*, 44,
952 73-91, 2019.

953 Cowardin, L. M., Carter, V., Golet, F. C., and LaRoe, E. T.: Classification of Wetlands and Deepwater
954 habitats of The United States, Fish and Wildlife Service, Washington DCFWS/OBS-79/31, 1979.

955 Creed, I. F., Lane, C. R., Serran, J. N., Alexander, L. C., Basu, N. B., Calhoun, A. J. K., Christensen, J.
956 R., Cohen, M. J., Craft, C., D'Amico, E., DeKeyser, E., Fowler, L., Golden, H. E., Jawitz, J. W., Kalla,
957 P., Kirkman, L. K., Lang, M., Leibowitz, S. G., Lewis, D. B., Marton, J., McLaughlin, D. L., Raanan-
958 Kiperwas, H., Rains, M. C., Rains, K. C., and Smith, L.: Enhancing protection for vulnerable waters,
959 *Nature Geoscience*, 10, 809-815, 10.1038/ngeo3041, 2017.

960 Cunha, D. G. F., Magri, R. A. F., Tromboni, F., Ranieri, V. E. L., Fendrich, A. N., Campanhão, L. M. B.,
961 Riveros, E. V., and Velázquez, J. A.: Landscape patterns influence nutrient concentrations in aquatic

962 systems: citizen science data from Brazil and Mexico, *Freshwater Science*, 38, 365-378,
963 10.1086/703396, 2019.

964 Dahl, T. E.: *Wetlands - Losses in the United States, 1780's to 1980's*, U.S. Department of Interior, Fish
965 and Wildlife Service Washington DC, 1990.

966 Davidson, N. C.: How much wetland has the world lost? Long-term and recent trends in global wetland
967 area, *Marine and Freshwater Research*, 65, 934-941, <http://dx.doi.org/10.1071/MF14173>, 2014.

968 Davidson, N. C., E. Fluet-Chouinard and C. M. Finlayson. 2018. Global extent and distribution of
969 wetlands: trends and issues. *Marine and Freshwater Research* 69, 4, 620-627, 2018.

970 De Groot, R., M. Stuij, M. Finlayson, and N. Davidson: *Valuing Wetlands: Guidance for Valuing the*
971 *Benefits Derived from Wetland Ecosystem Services*, Ramsar Convention Secretariat, Gland,
972 Switzerland and Secretariat of the Convention on Biological Diversity, Montreal, Canada, Gland,
973 Switzerland Ramsar Technical Report No. 3/CBD Technical Series No. 27, 2006.

974 DeVries, B., Huang, C., Lang, M., Jones, J., Huang, W., Creed, I., and Carroll, M.: *Automated*
975 *Quantification of Surface Water Inundation in Wetlands Using Optical Satellite Imagery*, *Remote*
976 *Sensing*, 9, 807, 2017.

977 Dewitz, J.: *National Land Cover Database (NLCD) 2016 Products: U.S. Geological Survey data release*
978 [dataset], <https://doi.org/10.5066/P96HHBIE>, 2019.

979 Drenkhan, F., Buytaert, W., Mackay, J. D., Barrand, N. E., Hannah, D. M., and Huggel, C.: Looking
980 beyond glaciers to understand mountain water security, *Nature Sustainability*, 10.1038/s41893-022-
981 00996-4, 2022.

982 ESA Worldwide Land Cover Mapping: <https://esa-worldcover.org/en>, last access: 22 December 2022.

983 ESA Land Cover CCI, Product User Guide Version 2.0:
984 https://maps.elie.ucl.ac.be/CCI/viewer/download/ESACCI-LC-Ph2-PUGv2_2.0.pdf, last access: May
985 2022.

986 ESRI World Terrain Base
987 <https://www.arcgis.com/home/item.html?id=be2e229ffc864c868a78f5ca68ca5b8e>, last accessed 22
988 December 2022.

989 Evenson, G. R., Golden, H. E., Lane, C. R., McLaughlin, D. L., and D'Amico, E.: Depressional Wetlands
990 Affect Watershed Hydrological, Biogeochemical, and Ecological Functions, *Ecological Applications*,
991 28, 953-966, 10.1002/eap.1701, 2018a.

992 Evenson, G. R., Jones, C. N., McLaughlin, D. L., Golden, H. E., Lane, C. R., DeVries, B., Alexander, L.
993 C., Lang, M. W., McCarty, G. W., and Sharifi, A.: A watershed-scale model for depressional wetland-
994 rich landscapes, *Journal of Hydrology X*, 1, 100002, <https://doi.org/10.1016/j.hydroa.2018.10.002>,
995 2018b.

996 Evenson, G. R., Golden, H. E., Christensen, J. R., Lane, C. R., Rajib, A., D'Amico, E., Mahoney, D. T.,
997 White, E., and Wu, Q.: Wetland restoration yields dynamic nitrate responses across the Upper
998 Mississippi river basin, *Environmental Research Communications*, 3, 095002, 10.1088/2515-
999 7620/ac2125, 2021.

1000 Fan, Y., Li, H., and Miguez-Macho, G.: Global Patterns of Groundwater Table Depth, *Science*, 339, 940-
1001 943, doi:10.1126/science.1229881, 2013.

1002 Fewtrell, T. J., Bates, P. D., Horritt, M., and Hunter, N. M.: Evaluating the effect of scale in flood
1003 inundation modelling in urban environments, *Hydrological Processes*, 22, 5107-5118,
1004 <https://doi.org/10.1002/hyp.7148>, 2008.

1005 Fluet-Chouinard, E., Lehner, B., Rebelo, L.-M., Papa, F., and Hamilton, S. K.: Development of a global
1006 inundation map at high spatial resolution from topographic downscaling of coarse-scale remote sensing
1007 data, *Remote Sensing of Environment*, 158, 348-361, <https://doi.org/10.1016/j.rse.2014.10.015>, 2015.

1008 Fluet-Chouinard, E., B. D. Stocker, Z. Zhang, A. Malhotra, J. R. Melton, B. Poulter, J. O. Kaplan, K. K.
1009 Goldewijk, S. Siebert, T. Minayeva, G. Hugelius, H. Joosten, A. Barthelmes, C. Prigent, F. Aires, A. M.
1010 Hoyt, N. Davidson, C. M. Finlayson, B. Lehner, R. B. Jackson and P. B. McIntyre. Extensive global
1011 wetland loss over the past three centuries, *Nature*, 614, 7947, 281-286, 2023.

1012 Fossey, M. and Rousseau, A. N.: Can isolated and riparian wetlands mitigate the impact of climate
1013 change on watershed hydrology? A case study approach, *Journal of Environmental Management*,
1014 184(2):327-339, <http://dx.doi.org/10.1016/j.jenvman.2016.09.043>, 2016.

1015 Golden, H. E., Lane, C. R., Rajib, A., and Wu, Q.: Improving global flood and drought predictions:
1016 integrating non-floodplain wetlands into watershed hydrologic models, *Environmental Research*
1017 *Letters*, 16, 091002, 10.1088/1748-9326/ac1fbc, 2021.

1018 Golden, H. E., Rajib, A., Lane, C. R., Christensen, J. R., Wu, Q., and Mengistu, S.: Non-floodplain
1019 Wetlands Affect Watershed Nutrient Dynamics: A Critical Review, *Environmental Science &*
1020 *Technology*, 53, 7203-7214, 10.1021/acs.est.8b07270, 2019.

1021 Golden, H. E., Sander, H. A., Lane, C. R., Zhao, C., Price, K., D'Amico, E., and Christensen, J. R.:
1022 Relative effects of geographically isolated wetlands on streamflow: a watershed-scale analysis,
1023 *Ecohydrology*, 9, 21-38, 10.1002/eco.1608, 2016.

1024 Golden, H. E., Creed, I. F., Ali, G., Basu, N. B., Neff, B. P., Rains, M. C., McLaughlin, D. L., Alexander,
1025 L. C., Ameli, A. A., Christensen, J. R., Evenson, G. R., Jones, C. N., Lane, C. R., and Lang, M.:
1026 Integrating geographically isolated wetlands into land management decisions, *Frontiers in Ecology and*
1027 *the Environment*, 15, 319-327, 10.1002/fee.1504, 2017.

1028 Gumbricht, T., Roman-Cuesta, R. M., Verchot, L., Herold, M., Wittmann, F., Householder, E., Herold,
1029 N., and Murdiyarso, D.: An expert system model for mapping tropical wetlands and peatlands reveals
1030 South America as the largest contributor, *Global Change Biology*, 23, 3581-3599,
1031 <https://doi.org/10.1111/gcb.13689>, 2017.

1032 Hamunyela, E., Hipondoka, M., Persendt, F., Sevelia Nghiyalwa, H., Thomas, C., and Matengu, K.:
1033 Spatio-temporal characterization of surface water dynamics with Landsat in endorheic Cuvelai-Etoshia
1034 Basin (1990–2021), *ISPRS Journal of Photogrammetry and Remote Sensing*, 191, 68-84,
1035 <https://doi.org/10.1016/j.isprsjprs.2022.07.007>, 2022.

1036 Hoch, J. M. and M. A. Trigg. Advancing global flood hazard simulations by improving comparability,
1037 benchmarking, and integration of global flood models. *Environmental Research Letters*, 14, 3, 034001,
1038 2019.

1039 Homer, C., Dewitz, J., Jin, S., Xian, G., Costello, C., Danielson, P., Gass, L., Funk, M., Wickham, J.,
1040 Stehman, S., Auch, R., and Riitters, K.: Conterminous United States land cover change patterns 2001–
1041 2016 from the 2016 National Land Cover Database, *ISPRS Journal of Photogrammetry and Remote*
1042 *Sensing*, 162, 184-199, <https://doi.org/10.1016/j.isprsjprs.2020.02.019>, 2020.

1043 Horritt, M. S. and Bates, P. D.: Evaluation of 1D and 2D numerical models for predicting river flood
1044 inundation, *Journal of Hydrology*, 268, 87-99, [http://dx.doi.org/10.1016/S0022-1694\(02\)00121-X](http://dx.doi.org/10.1016/S0022-1694(02)00121-X),
1045 2002.

1046 Hu, S., Niu, Z., and Chen, Y.: Global Wetland Datasets: a Review, *Wetlands*, 37, 807-817,
1047 [10.1007/s13157-017-0927-z](https://doi.org/10.1007/s13157-017-0927-z), 2017a.

1048 Hu, S., Niu, Z., Chen, Y., Li, L., and Zhang, H.: Global wetlands: Potential distribution, wetland loss, and
1049 status, *Science of The Total Environment*, 586, 319-327,
1050 <http://dx.doi.org/10.1016/j.scitotenv.2017.02.001>, 2017b.

1051 Huang, W., DeVries, B., Huang, C., Lang, M., Jones, J., Creed, I., and Carroll, M.: Automated Extraction
1052 of Surface Water Extent from Sentinel-1 Data, *Remote Sensing*, 10, 797, 2018.

1053 IPCC: Intergovernmental Panel on Climate Change 2014: Impacts, adaptation, and vulnerability,
1054 Cambridge University Press, Cambridge, U.K.2014.

1055 Jafarzadegan, K., Merwade, V., and Saksena, S.: A geomorphic approach to 100-year floodplain mapping
1056 for the Conterminous United States, *Journal of Hydrology*, 561, 43-58,
1057 <https://doi.org/10.1016/j.jhydrol.2018.03.061>, 2018.

1058 Jakubínský, J., Prokopová, M., Raška, P., Salvati, L., Bezak, N., Cudlín, O., Cudlín, P., Purkyt, J., Vezza,
1059 P., Camporeale, C., Daněk, J., Pástor, M., and Lepeška, T.: Managing floodplains using nature-based
1060 solutions to support multiple ecosystem functions and services, *WIREs Water*, 8, e1545,
1061 <https://doi.org/10.1002/wat2.1545>, 2021.

1062 Jin, S., Homer, C., Yang, L., Danielson, P., Dewitz, J., Li, C., Zhu, Z., Xian, G., and Howard, D.: Overall
1063 Methodology Design for the United States National Land Cover Database 2016 Products, Remote
1064 Sensing, 11, 2971, 2019.

1065 Jones, C. N., Evenson, G. R., McLaughlin, D. L., Vanderhoof, M. K., Lang, M. W., McCarty, G. W.,
1066 Golden, H. E., Lane, C. R., and Alexander, L. C.: Estimating restorable wetland water storage at
1067 landscape scales, Hydrological Processes, 32, 305-313, 10.1002/hyp.11405, 2018.

1068 Karra, K., Kontgis, C., Statman-Weil, Z., Mazzariello, J. C., Mathis, M., & Brumby, S. P. Global land
1069 use/land cover with Sentinel 2 and deep learning. In: 2021 IEEE International Geoscience and Remote
1070 Sensing Symposium IGARSS (pp. 4704-4707). IEEE, doi.org/10.1109/IGARSS47720.2021.9553499,
1071 2021.

1072 Kam, S. P.: Valuing the role of living aquatic resources to rural livelihoods in multiple-use, seasonally-
1073 inundated wetlands in the Yellow River Basin of China, for improved governance, CGIAR Challenge
1074 Program on Water & Food, Colombo, Sri Lanka, <https://hdl.handle.net/10568/3859>, 2010.

1075 Kremenetski, K. V., Velichko, A. A., Borisova, O. K., MacDonald, G. M., Smith, L. C., Frey, K. E., and
1076 Orlova, L. A.: Peatlands of the Western Siberian lowlands: current knowledge on zonation, carbon
1077 content and Late Quaternary history, Quaternary Science Reviews, 22, 703-723, 2003.

1078 Kundzewicz, Z. W., Hegger, D. L. T., Matczak, P., and Driessen, P. P. J.: Opinion: Flood-risk reduction:
1079 Structural measures and diverse strategies, Proceedings of the National Academy of Sciences, 115,
1080 12321-12325, 10.1073/pnas.1818227115, 2018.

1081 Lane, C. R. and D'Amico, E.: Identification of Putative Geographically Isolated Wetlands of the
1082 Conterminous United States, JAWRA Journal of the American Water Resources Association, 52, 705-
1083 722, 10.1111/1752-1688.12421, 2016.

1084 Lane, C. R., Leibowitz, S. G., Autrey, B. C., LeDuc, S. D., and Alexander, L. C.: Hydrological, Physical,
1085 and Chemical Functions and Connectivity of Non-Floodplain Wetlands to Downstream Waters: A
1086 Review, JAWRA Journal of the American Water Resources Association, 54, 346-371, 10.1111/1752-
1087 1688.12633, 2018.

1088 Lane, C. R., Creed, I. F., Golden, H. E., Leibowitz, S. G., Mushet, D. M., Rains, M. C., Wu, Q.,
1089 D'Amico, E., Alexander, L. C., Ali, G. A., Basu, N. B., Bennett, M. G., Christensen, J. R., Cohen, M.
1090 J., Covino, T. P., DeVries, B., Hill, R. A., Jencso, K., Lang, M. W., McLaughlin, D. L., Rosenberry, D.
1091 O., Rover, J., and Vanderhoof, M. K.: Vulnerable Waters are Essential to Watershed Resilience,
1092 Ecosystems, 10.1007/s10021-021-00737-2, 2022.

1093 Lane, C. R., E. D'Amico, J. R. Christensen, H. E. Golden, Q. Wu, and A. Rajib. Global non-floodplain
1094 wetlands [dataset], https://gaftp.epa.gov/EPADDataCommons/ORD/Global_NonFloodplain_Wetlands/
1095 and <https://doi.org/10.23719/1528331>, 2023.

1096 Lehner, B. and Doll, P.: Development and validation of a global database of lakes, reservoirs and
1097 wetlands, *Journal of Hydrology*, 296, 1-22, 2004.

1098 Lehner, B. and Grill, G.: Global river hydrography and network routing: baseline data and new
1099 approaches to study the world's large river systems, *Hydrological Processes*, 27, 2171-2186,
1100 <https://doi.org/10.1002/hyp.9740>, 2013.

1101 Leibowitz, S.: Geographically Isolated Wetlands: Why We Should Keep the Term, *Wetlands*, 35, 997-
1102 1003, 10.1007/s13157-015-0691-x, 2015.

1103 Leibowitz, S. G.: Isolated wetlands and their functions: an ecological perspective, *Wetlands*, 22, 517-531,
1104 2003.

1105 Leibowitz, S. G., Hill, R. A., Creed, I. F., Compton, J. E., Golden, H. E., Weber, M. H., Rains, M. C.,
1106 Jones, J., C. E., Lee, E. H., Christensen, J. R., Bellmore, R. A., and Lane, C. R.: Connections matter:
1107 National classification links wetlands and water quality, *Science*, In Review.

1108 Liu, D., Cao, C., Chen, W., Ni, X., Tian, R., and Xing, X.: Monitoring and predicting the degradation of a
1109 semi-arid wetland due to climate change and water abstraction in the Ordos Larus relictus National
1110 Nature Reserve, China, *Geomatics, Natural Hazards and Risk*, 8, 367-383,
1111 10.1080/19475705.2016.1220024, 2017.

1112 Makungu, E. and Hughes, D. A.: Understanding and modelling the effects of wetland on the hydrology
1113 and water resources of large African river basins, *Journal of Hydrology*, 603, 127039,
1114 <https://doi.org/10.1016/j.jhydrol.2021.127039>, 2021.

1115 Martinis, S., Groth, S., Wieland, M., Knopp, L., and Rättich, M.: Towards a global seasonal and
1116 permanent reference water product from Sentinel-1/2 data for improved flood mapping, *Remote
1117 Sensing of Environment*, 278, 113077, <https://doi.org/10.1016/j.rse.2022.113077>, 2022.

1118 Marton, J. M., Creed, I. F., Lewis, D., Lane, C. R., Basu, N., Cohen, M. J., and C., C.: Geographically
1119 isolated wetlands are important biogeochemical reactors on the landscape, *BioScience*, 65, 408-418,
1120 10.1093/biosci/biv009, 2015.

1121 McCauley, L. A., Anteau, M. J., van der Burg, M. P., and Wiltermuth, M. T.: Land use and wetland
1122 drainage affect water levels and dynamics of remaining wetlands, *Ecosphere*, 6, art92, 10.1890/ES14-
1123 00494.1, 2015.

1124 McKenna, O. P., Mushet, D. M., Rosenberry, D. O., and LaBaugh, J. W.: Evidence for a climate-induced
1125 ecohydrological state shift in wetland ecosystems of the southern Prairie Pothole Region, *Climatic
1126 Change*, 145, 273-287, 10.1007/s10584-017-2097-7, 2017.

1127 McLaughlin, D. L., Kaplan, D. A., and Cohen, M. J.: A significant nexus: Geographically isolated
1128 wetlands influence landscape hydrology, *Water Resources Research*, 50, 7153-7166,
1129 10.1002/2013WR015002, 2014.

1130 Merken, R., Deboelpaep, E., Teunen, J., Saura, S., and Koedam, N.: Wetland Suitability and Connectivity
1131 for Trans-Saharan Migratory Waterbirds, *PLOS ONE*, 10, e0135445, 10.1371/journal.pone.0135445,
1132 2015.

1133 Messenger, M. L., Lehner, B., Grill, G., Nedeva, I., and Schmitt, O.: Estimating the volume and age of
1134 water stored in global lakes using a geo-statistical approach, *Nature Communications*, 7, 13603,
1135 10.1038/ncomms13603, 2016.

1136 Mudashiru, R. B., N. Sabtu, I. Abustan and W. Balogun. Flood hazard mapping methods: A review.
1137 Journal of Hydrology, 603, 126846, 2021.

1138 Mushet, D., Calhoun, A., Alexander, L., Cohen, M., DeKeyser, E., Fowler, L., Lane, C., Lang, M., Rains,
1139 M., and Walls, S.: Geographically Isolated Wetlands: Rethinking a Misnomer, Wetlands, 35, 423-431,
1140 10.1007/s13157-015-0631-9, 2015.

1141 Mushet, D. M., Alexander, L. C., Bennett, M., Schofield, K., Christensen, J. R., Ali, G., Pollard, A., Fritz,
1142 K., and Lang, M. W.: Differing Modes of Biotic Connectivity within Freshwater Ecosystem Mosaics,
1143 JAWRA Journal of the American Water Resources Association, 55, 307-317, 10.1111/1752-
1144 1688.12683, 2019.

1145 Nardi, F., Annis, A., Di Baldassarre, G., Vivoni, E. R., and Grimaldi, S.: GFPLAIN250m, a global high-
1146 resolution dataset of Earth's floodplains, Scientific Data, 6, 180309, 10.1038/sdata.2018.309, 2019.

1147 National Landcover Database (NLCD) 2019 NLCD Land Cover (CONUS), <https://www.mrlc.gov/data>,
1148 last accessed 22 December 2022.

1149 Nitzsche, K. N., Kalettka, T., Premke, K., Lischeid, G., Gessler, A., and Kayler, Z. E.: Land-use and
1150 hydroperiod affect kettle hole sediment carbon and nitrogen biogeochemistry, Science of The Total
1151 Environment, 574, 46-56, <http://dx.doi.org/10.1016/j.scitotenv.2016.09.003>, 2017.

1152 Olefeldt, D., Hovemyr, M., Kuhn, M. A., Bastviken, D., Bohn, T. J., Connolly, J., Crill, P., Euskirchen, E.
1153 S., Finkelstein, S. A., Genet, H., Grosse, G., Harris, L. I., Heffernan, L., Helbig, M., Hugelius, G.,
1154 Hutchins, R., Juutinen, S., Lara, M. J., Malhotra, A., Manies, K., McGuire, A. D., Natali, S. M.,
1155 O'Donnell, J. A., Parmentier, F. J. W., Räsänen, A., Schädel, C., Sonntag, O., Strack, M., Tank, S. E.,
1156 Treat, C., Varner, R. K., Virtanen, T., Warren, R. K., and Watts, J. D.: The Boreal–Arctic Wetland and
1157 Lake Dataset (BAWLD), Earth Syst. Sci. Data, 13, 5127-5149, 10.5194/essd-13-5127-2021, 2021.

1158 Pappenberger, F., E. Dutra, F. Wetterhall and H. L. Cloke. Deriving global flood hazard maps of fluvial
1159 floods through a physical model cascade. Hydrol. Earth Syst. Sci., 16, 11, 4143-4156, 2012.

1160 Pekel, J.-F., Cottam, A., Gorelick, N., and Belward, A. S.: High-resolution mapping of global surface
1161 water and its long-term changes, *Nature*, 540, 418-422, 10.1038/nature20584, 2016.

1162 Prigent, C., Papa, F., Aires, F., Rossow, W. B., and Matthews, E.: Global inundation dynamics inferred
1163 from multiple satellite observations, 1993–2000, *Journal of Geophysical Research: Atmospheres*, 112,
1164 <https://doi.org/10.1029/2006JD007847>, 2007.

1165 PRISM Climate Group, Parameter-elevation Regressions on Independent Slopes Model,
1166 prism.oregonstate.edu/, last accessed 22 December 2022.

1167 Rains, M. C., Leibowitz, S. G., Cohen, M. J., Creed, I. F., Golden, H. E., Jawitz, J. W., Kalla, P., Lane, C.
1168 R., Lang, M. W., and McLaughlin, D. L.: Geographically isolated wetlands are part of the hydrological
1169 landscape, *Hydrological Processes*, 30, 153-160, 10.1002/hyp.10610, 2016.

1170 Rajib, A., Golden, H. E., Lane, C. R., and Wu, Q.: Surface depression and wetland water storage
1171 improves major river basin hydrologic predictions, *Water Resources Research*, 56, e2019WR026561,
1172 <https://doi.org/10.1029/2019WR026561>, 2020.

1173 Rajib, A., Zheng, Q., Golden, H. E., Wu, Q., Lane, C. R., Christensen, J. R., Morrison, R. R., Annis, A.,
1174 and Nardi, F.: The changing face of floodplains in the Mississippi River Basin detected by a 60-year
1175 land use change dataset, *Scientific Data*, 8, 271, 10.1038/s41597-021-01048-w, 2021.

1176 Robarts, R., Zhulidov, A., and Pavlov, D.: The State of knowledge about wetlands and their future under
1177 aspects of global climate change: the situation in Russia, *Aquatic Sciences*, 75, 27-38, 10.1007/s00027-
1178 011-0230-7, 2013.

1179 Rodrigues, L. N., Sano, E. E., Steenhuis, T. S., and Passo, D. P.: Estimation of Small Reservoir Storage
1180 Capacities with Remote Sensing in the Brazilian Savannah Region, *Water Resources Management*, 26,
1181 873-882, 10.1007/s11269-011-9941-8, 2012.

1182 Rodríguez-Rodríguez, M., Aguilera, H., Guardiola-Albert, C., and Fernández-Ayuso, A.: Climate
1183 Influence Vs. Local Drivers in Surface Water-Groundwater Interactions in Eight Ponds of Doñana
1184 National Park (Southern Spain), *Wetlands*, 41, 25, 10.1007/s13157-021-01425-6, 2021.

1185 Rudari, R., Silvestro, F., Campo, L., Rebora, N., Boni, G., and Herold, C. Improvement of the global
1186 flood model for the GAR 2015. United Nations Office for Disaster Risk Reduction (UNISDR), Centro
1187 Internazionale in Monitoraggio Ambientale (CIMA), UNEP GRID-Arendal (GRID-Arendal): Geneva,
1188 Switzerland, 69, 2015.

1189 Sampson, C. C., Smith, A. M., Bates, P. D., Neal, J. C., Alfieri, L., and Freer, J. E.: A high-resolution
1190 global flood hazard model, *Water Resources Research*, 51, 7358-7381, 10.1002/2015WR016954, 2015.

1191 Samways, M. J., Deacon, C., Kietzka, G. J., Pryke, J. S., Vorster, C., and Simaika, J. P.: Value of
1192 artificial ponds for aquatic insects in drought-prone southern Africa: a review, *Biodiversity and
1193 Conservation*, 29, 3131-3150, 10.1007/s10531-020-02020-7, 2020.

1194 Sangwan, N. and Merwade, V.: A Faster and Economical Approach to Floodplain Mapping Using Soil
1195 Information, *JAWRA Journal of the American Water Resources Association*, 51, 1286-1304,
1196 10.1111/1752-1688.12306, 2015.

1197 Schofield, K. A., Alexander, L. C., Ridley, C. E., Vanderhoof, M. K., Fritz, K. M., Autrey, B. C.,
1198 DeMeester, J. E., Kepner, W. G., Lane, C. R., Leibowitz, S. G., and Pollard, A. I.: Biota Connect
1199 Aquatic Habitats throughout Freshwater Ecosystem Mosaics, *JAWRA Journal of the American Water
1200 Resources Association*, 54, 372-399, 10.1111/1752-1688.12634, 2018.

1201 Serran, J. N., Creed, I. F., Ameli, A. A., and Aldred, D. A.: Estimating rates of wetland loss using power-
1202 law functions, *Wetlands*, 38, 109-120, 10.1007/s13157-017-0960-y, 2017.

1203 Shaw, D. A., Vanderkamp, G., Conly, F. M., Pietroniro, A., and Martz, L.: The Fill–Spill Hydrology of
1204 Prairie Wetland Complexes during Drought and Deluge, *Hydrological Processes*, 26, 3147-3156,
1205 10.1002/hyp.8390, 2012.

1206 Smith, L. L., Subalusky, A. L., Atkinson, C. L., Earl, J. E., Mushet, D. M., Scott, D. E., Lance, S. L., and
1207 Johnson, S. A.: Biological Connectivity of Seasonally Poned Wetlands across Spatial and Temporal
1208 Scales, *JAWRA Journal of the American Water Resources Association*, 55, 334-353, 10.1111/1752-
1209 1688.12682, 2019.

1210 Strahler, A. N.: Quantitative analysis of watershed geomorphology, American Geophysical Union
1211 Transactions, 38, 913-920, 1957.

1212 Sullivan, S. M. P., Rains, M. C., and Rodewald, A. D.: Opinion: The proposed change to the definition of
1213 “waters of the United States” flouts sound science, Proceedings of the National Academy of Sciences,
1214 116, 11558, 10.1073/pnas.1907489116, 2019.

1215 Tayefi, V., Lane, S. N., Hardy, R. J., and Yu, D.: A comparison of one- and two-dimensional approaches
1216 to modelling flood inundation over complex upland floodplains, Hydrological Processes, 21, 3190-
1217 3202, 10.1002/hyp.6523, 2007.

1218 Tootchi, A., Jost, A., and Ducharme, A.: Multi-source global wetland maps combining surface water
1219 imagery and groundwater constraints, Earth Syst. Sci. Data, 11, 189-220, 10.5194/essd-11-189-2019,
1220 2019.

1221 Tsendbazar, N., Herold, M., Li, L., Tarko, A., de Bruin, S., Masiliunas, D., Lesiv, M., Fritz, S., Buchhorn,
1222 M., Smets, B., Van De Kerchove, R., and Duerauer, M.: Towards operational validation of annual
1223 global land cover maps, Remote Sensing of Environment, 266, 112686,
1224 <https://doi.org/10.1016/j.rse.2021.112686>, 2021.

1225 Tullos, D.: Opinion: How to achieve better flood-risk governance in the United States, Proceedings of the
1226 National Academy of Sciences, 115, 3731-3734, 10.1073/pnas.1722412115, 2018.

1227 Uden, D. R., Allen, C. R., Bishop, A. A., Grosse, R., Jorgensen, C. F., LaGrange, T. G., Stutheit, R. G.,
1228 and Vrtiska, M. P.: Predictions of future ephemeral springtime waterbird stopover habitat availability
1229 under global change, Ecosphere, 6, 1-26, 10.1890/ES15-00256.1, 2015.

1230 United States Geological Survey (USGS) National Elevation Dataset, [https://www.usgs.gov/3d-elevation-](https://www.usgs.gov/3d-elevation-program)
1231 [program](https://www.usgs.gov/3d-elevation-program), last accessed 22 December 2022.

1232 United States Geological Survey (USGS) Watershed Boundary Dataset, [https://www.usgs.gov/national-](https://www.usgs.gov/national-hydrography/access-national-hydrography-products)
1233 [hydrography/access-national-hydrography-products](https://www.usgs.gov/national-hydrography/access-national-hydrography-products), last accessed 22 December 2022.

1234 Van Meter, K. J. and Basu, N. B.: Signatures of human impact: size distributions and spatial organization
1235 of wetlands in the Prairie Pothole landscape, *Ecological Applications*, 25, 451-465, 10.1890/14-0662.1,
1236 2015.

1237 Van Meter, K. J., Basu, N. B., Tate, E., and Wyckoff, J.: Monsoon Harvests: The Living Legacies of
1238 Rainwater Harvesting Systems in South India, *Environmental Science & Technology*, 48, 4217-4225,
1239 10.1021/es4040182, 2014.

1240 Vanderhoof, M. K. and Lane, C. R.: The potential role of very high-resolution imagery to characterise
1241 lake, wetland and stream systems across the Prairie Pothole Region, United States, *International Journal*
1242 *of Remote Sensing*, 40, 5768-5798, 10.1080/01431161.2019.1582112, 2019.

1243 Wania, R., Melton, J. R., Hodson, E. L., Poulter, B., Ringeval, B., Spahni, R., Bohn, T., Avis, C. A.,
1244 Chen, G., Eliseev, A. V., Hopcroft, P. O., Riley, W. J., Subin, Z. M., Tian, H., van Bodegom, P. M.,
1245 Kleinen, T., Yu, Z. C., Singarayer, J. S., Zürcher, S., Lettenmaier, D. P., Beerling, D. J., Denisov, S. N.,
1246 Prigent, C., Papa, F., and Kaplan, J. O.: Present state of global wetland extent and wetland methane
1247 modelling: methodology of a model inter-comparison project (WETCHIMP), *Geosci. Model Dev.*, 6,
1248 617-641, 10.5194/gmd-6-617-2013, 2013.

1249 Werner, M. G. F., Hunter, N. M., and Bates, P. D.: Identifiability of distributed floodplain roughness
1250 values in flood extent estimation, *Journal of Hydrology*, 314, 139-157,
1251 <https://doi.org/10.1016/j.jhydrol.2005.03.012>, 2005.

1252 Wickham, J., Stehman, S. V., Sorenson, D. G., Gass, L., and Dewitz, J. A.: Thematic accuracy assessment
1253 of the NLCD 2016 land cover for the conterminous United States, *Remote Sensing of Environment*,
1254 257, 112357, <https://doi.org/10.1016/j.rse.2021.112357>, 2021.

1255 Wing, O. E. J., Bates, P. D., Sampson, C. C., Smith, A. M., Johnson, K. A., and Erickson, T. A.:
1256 Validation of a 30 m resolution flood hazard model of the conterminous United States, *Water Resources*
1257 *Research*, 53, 7968-7986, 10.1002/2017WR020917, 2017.

1258 Winsemius, H. C., L. P. H. Van Beek, B. Jongman, P. J. Ward and A. Bouwman. A framework for global
1259 river flood risk assessments, *Hydrol. Earth Syst. Sci.*, 17, 5, 1871-1892, 2013.

1260 Winter, T. C.: The Vulnerability of Wetlands to Climate Change: A Hydrologic Landscape Perspective,
1261 JAWRA Journal of the American Water Resources Association, 36, 305-311, 10.1111/j.1752-
1262 1688.2000.tb04269.x, 2000.

1263 Winter, T. C., J.W. Harvey, O.L. Franke, and Alley, W. M.: Ground Water and Surface Water: A Single
1264 Resoure, U.S. Government Printing Office, Washington, DC., 1998.

1265 Woznicki, S. A., Baynes, J., Panlasigui, S., Mehaffey, M., and Neale, A.: Development of a spatially
1266 complete floodplain map of the conterminous United States using random forest, Science of The Total
1267 Environment, 647, 942-953, <https://doi.org/10.1016/j.scitotenv.2018.07.353>, 2019.

1268 Wu, Q., Lane, C. R., Wang, L., Vanderhoof, M. K., Christensen, J. R., and Liu, H.: Efficient Delineation
1269 of Nested Depression Hierarchy in Digital Elevation Models for Hydrological Analysis Using Level-Set
1270 Method, JAWRA Journal of the American Water Resources Association, 55, 354-368, 10.1111/1752-
1271 1688.12689, 2019a.

1272 Wu, Q., Lane, C. R., Li, X., Zhao, K., Zhou, Y., Clinton, N., DeVries, B., Golden, H. E., and Lang, M.
1273 W.: Integrating LiDAR data and multi-temporal aerial imagery to map wetland inundation dynamics
1274 using Google Earth Engine, Remote Sensing of Environment, 228, 1-13,
1275 <https://doi.org/10.1016/j.rse.2019.04.015>, 2019b.

1276 Xi, Y., Peng, S., Ducharne, A., Ciais, P., Gumbricht, T., Jimenez, C., Poulter, B., Prigent, C., Qiu, C.,
1277 Saunois, M., and Zhang, Z.: Gridded maps of wetlands dynamics over mid-low latitudes for 1980–2020
1278 based on TOPMODEL, Scientific Data, 9, 347, 10.1038/s41597-022-01460-w, 2022.

1279 Yamazaki, D., S. Kanae, H. Kim and T. Oki. A physically based description of floodplain inundation
1280 dynamics in a global river routing model, Water Resources Research, 47, 4, 2011.

1281 Yamazaki, D., Ikeshima, D., Sosa, J., Bates, P. D., Allen, G., and Pavelsky, T.: MERIT Hydro: A high-
1282 resolution global hydrography map based on latest topography datasets, Water Resources Research, 55,
1283 5053-5073, 10.1029/2019wr024873, 2019.

1284 Zanaga, D., Van De Kerchove, R., De Keersmaecker, W., Souverijns, N., Brockmann, C., Quast, R.,
1285 Wevers, J., Grosu, A., Paccini, A., Vergnaud, S., Cartus, O., Santoro, M., Fritz, S., Georgieva, I., Lesiv,

1286 M., Carter, S., Herold, M., Li, Linlin, Tsendbazar, N.E., Ramoïno, F., Arino, O.: ESA WorldCover 10
1287 m 2020 v100, <https://doi.org/10.5281/zenodo.5571936> 2021.

1288 Zedler, J. B. and Kercher, S.: Causes and consequences of invasive plants in wetlands: Opportunities,
1289 opportunists, and outcomes, *Critical Reviews in Plant Sciences*, 23, 431-452, 2004.

1290 Zhang, X., L. Liu, T. Zhao, X. Chen, S. Lin, J. Wang, J. Mi and W. Liu. GWL_FCS30: global 30 m
1291 wetland map with fine classification system using multi-sourced and time-series remote sensing
1292 imagery in 2020. *Earth Syst. Sci. Data* 15, 265-293, 2023.

1293 Zhu, Y., Xu, Y., Deng, X., Kwon, H., and Qin, Z.: Peatland Loss in Southeast Asia Contributing to U.S.
1294 Biofuel's Greenhouse Gas Emissions, *Environmental Science & Technology*, 10.1021/acs.est.2c01561,
1295 2022.

1296